Paraglacial rock-slope failure following deglaciation in western Norway

Alastair M. Curry

Department of Biological and Environmental Sciences, University of Hertfordshire, College Lane, Hatfield, Hertfordshire AL10 9AB, U.K.
a.curry4@herts.ac.uk

Abstract

The paraglacial framework describes the geomorphological response to glaciation and deglaciation, whereby non-renewable, metastable, glacially-conditioned sediment sources are progressively released by a range of nonglacial processes. These include slope failures that directly modify the bedrock topography of mountain landscapes. This chapter synthesises recent research on the paraglacial evolution of western Norway's mountain rock-slopes, and evaluates the importance of glaciation, deglaciation, and associated climatic and non-climatic processes. Following an introduction to the concept of paraglacial landscape change, current understanding of rock-slope responses to deglaciation are outlined, focussing on the spatial distribution, timing, duration and causes of rock-slope failure activity. Preliminary analysis of an inventory of published ages for 49 prehistoric, moderate-large (>10^3 m^3) rock-slope failures (RSFs) indicates that the great majority occurred in the Late Weichselian / Early Holocene transition (~13-9 ka), within 2 ka of deglaciation. Subsequent RSFs were much smaller, though event frequency increased again at 8-7 ka and 5-4 ka BP. The majority of RSFs were not directly triggered by deglaciation (debuttressing) but were preconditioned for more than 1000 years after ice withdrawal, until slopes collapsed. It is proposed that the primary causes of failure within 2 ka of ice retreat were stress redistribution, subcritical fracture propagation, with some events possibly triggered by seismic activity. While earthquakes may have triggered renewed failure of rock-slopes in the Late Holocene, it seems likely that permafrost degradation and water supply were locally important. Priority avenues for further research are briefly identified.

Keywords

paraglacial, rock-slope failure, glaciation, deglaciation, rockfall, rock avalanche, stress-release

5.1 Introduction

Rock slope failures (RSFs) are often located close to retreating mountain glaciers, dominating bedrock erosion and sediment distributions in alpine landscapes, and representing a hazard to mountain communities and resources. Understanding the distribution, timing and duration of rock-slope activity is critically important for accurately reconstructing Quaternary landscape evolution and sediment flux, and managing hazard risks in glaciated areas.

Definition and scope

This chapter reviews current understanding of the legacy of glaciation on the failure of rock slopes in western Norway's mountain landscape. The act of failure usually involves the initial formation of a fully developed rupture surface as a displacement or strain discontinuity (Hungr et al. 2014), though this may be preceded by rock-slope deformation (rock-slope instability). Both phenomena are on a continuum, and many RSFs exhibit both. Here, 'rock-slope failure' is used as an overall umbrella term to refer to "any substantial rock-mass exposed to slope gravitational processes which has lost structural integrity, regardless of its degree of disintegration or distance travelled" (Jarman and Harrison 2019, p. 202). Accordingly, RSFs reflect a range of mechanisms that directly displace *in situ* bedrock, and include rock slides (that may develop into rock avalanches), rock-slope deformations, rock topples and falls (McColl, 2014).

After introducing the reader to the concept of paraglacial landscape adjustment and the study area, following sections highlight the most important characteristics with reference to deglaciated rock-slopes in western Norway, including the processes, spatial distribution, timing, periodicity and causes of rock-slope failure in the region. Promising avenues for future research are briefly highlighted, and principal findings are summarised.

Unless otherwise indicated, radiometric ^{14}C ages have been calibrated to calendar (cal.) years before present using the IntCal13 dataset (Reimer et al. 2013), and average ^{10}Be exposure ages are also given in years before present.

Paraglacial landscape change

While geomorphologists have long recognised how landscapes may be influenced by glaciation and deglaciation, specific consideration of the transitional, 'paraglacial' adjustment of a landscape to nonglacial conditions is relatively new (Ryder 1971). The term 'paraglacial' highlights "non-glacial processes that are directly conditioned by glaciation" (Church and Ryder 1972, p. 3059) in proglacial and ice-marginal settings. Early use of the paraglacial concept focussed primarily on the abrupt and radical change in terrestrial fluvial entrainment and sedimentation associated with Late Pleistocene or Early Holocene deglaciation, whereby vast quantities of unconsolidated glacigenic detritus became liable to enhanced erosion, reworking and redeposition by rivers and debris flows, manifest in the accumulation of impressive fans and valley fills within millennia of deglaciation.

More recently, however, the notion of paraglacial landscape change has been applied to a wide range of non-glacial processes, landforms, landsystems and deposits conditioned by both Pleistocene and present-day glaciation and deglaciation within diverse geomorphological contexts over a range of process and spatial scales. In particular, since the mid-1980s the concept of paraglacial landscape adjustment (or relaxation) from a glacially conditioned state to non-glacial conditions has been increasingly recognised as being of critical importance in understanding postglacial landscape evolution and its theoretical framework, as well as predicting landform response to current and future environmental change.

Following widespread deglaciation, the sediment budgets of a variety of landscape subsystems may be characterised by a state of disequilibrium. In rock-slope landsystems, for example, rockwalls may progressively weaken and eventually fail in response to glacier thinning and locally induced stress changes, variations in temperature and moisture, or as a result of seismicity associated with glacio-isostatic adjustment. Release of such sediments may be conceptualized as a sediment cascade (Ballantyne 2002a), in which transport of sediment from non-renewable, glacially-conditioned metastable sources is stored for varying timescales in a range of landforms and deposits such as talus accumulations, landslide debris and fjord deposits (referred to collectively as accommodation space (Brierley 2010)).

While there is nothing unique about the paraglacial environment or paraglacial processes *per se*, one of the most fruitful aspects of this research lies in recognising and interpreting the 'paraglacial period'. This temporal adjustment is characterised by high rates of glacially-

conditioned sediment release that peak soon after the land surface emerges from retreating glacier ice, when unstable or metastable sediment stores are exposed and subsequently depleted by a wide range of processes (Fig. 5.1). The idea of paraglacial landscape response was first considered a unique episode of rapid readjustment in the evolution of formerly glacierised landscapes (André 2009; Slaymaker 2009), however, it has subsequently developed into a unifying, dynamic systems concept, illustrated for example, by steady-state and exhaustion models (Fig. 5.1b) of sediment release and storage (Cruden and Hu 1993; Ballantyne 2002a, b; Cossart and Fort 2008; Ballantyne and Stone 2013). During deglaciation, primary sediment flux rates are predicted to increase rapidly then decline towards background nonglacial denudation rates, the rate of decline (and duration of the paraglacial period) being controlled by sediment availability and stability.

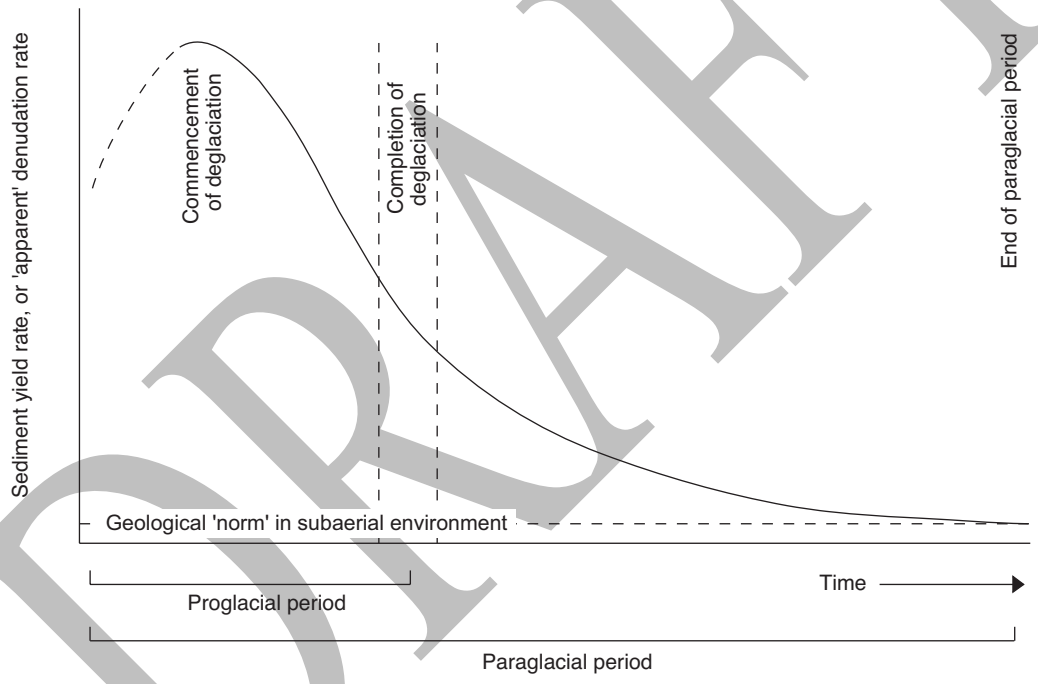

Fig. 5.1. The paraglacial period: conceptual representation of the pattern of glacially-conditioned sediment release and reworking, as envisaged by Church and Ryder (1972). Deglaciation marks the onset of this period of enhanced sediment yield which terminates when sediment yield has declined to long-term subaerial denudation norms.

Such an orderly, monotonic evolution is commonly disrupted, however, by extrinsic perturbations, transient storage, lags and feedbacks in the sediment-transport system, and reworking of secondary paraglacial stores, leading to delayed, renewed and rejuvenated reworking of glacially-conditioned sediment (Ballantyne 2003; Knight and Harrison 2018).

Accordingly, different geomorphic systems exhibit paraglacial relaxation over widely differing timescales, with the duration of rock-slope system responses to deglaciation measured in terms of millennia. Moreover, the trajectory and rate of response and recovery are dependent on the pre-existing system state, the extent of the glacial disturbance, and spatial scale (Church and Slaymaker 1989; Slaymaker 2011), implying that individual rock-slope subsystems may attain adjustment with their non-glacial environment while mountain range systems are still in recovery mode.

This persistence of landscape memory is widely evident. Many areas deglaciated in the Late Pleistocene can be regarded as having not yet fully adjusted to nonglacial conditions, at least in terms of glacially-conditioned sediment supply, and many landforms in these areas are out of equilibrium with both former glacial, and contemporary nonglacial conditions. If this is the case, then the development of most formerly glaciated landscapes can be regarded as transitional or transient, rather than linear (Church 2002; Hewitt 2002; Slaymaker 2009, 2011). Paraglaciation (the collective and cumulative effects of paraglacial rates of activity in modifying the landscape) hereby represents system recovery following glacial disturbance (Hewitt 2006; Slaymaker 2009), where a transitional, disturbance regime landscape persists until glacially-conditioned sediment sources either become exhausted or stable.

The temporal pattern of paraglacial recovery is further complicated by Neoglaciation, the waxing and waning of Holocene glaciers in upper source areas, as periods of localised glacial retreat result in the exposure of fresh metastable sediments. Rapid shrinkage of mountain and arctic glaciers during the 20th and 21st centuries has also resulted in widespread exposure of deglaciated terrain.

While no preserved analogues exist for the climatic contexts envisaged under future, anthropogenically-enhanced global warming, the paraglacial response to recent deglaciation arguably provides a valuable template for predicting how contemporary paraglacial systems in sensitive glaciated mountain environments may respond to future changes. As deglaciation gathers pace in high-altitude and high-latitude regions presently experiencing increased sediment flux, a major priority is to better understand the trajectory and behaviour of paraglaciation. Indeed, Knight and Harrison (2014, p. 256) claim that the increasing dominance of the paraglacial process domain in mid- to high-latitude glaciated mountains this

century will represent “the most significant and fastest change to take place in mountain cryosystems in at least the last 9000 years”.

The following section focuses specifically on the response of rock-slope systems to glaciation and deglaciation.

5.2 Paraglacial rock-slope adjustment: overview

Many authors have proposed a causal connection between deglaciation of steep, glacially-modified rockwalls and subsequent RSF activity, associated with both recent glacier retreat (McSaveney 1993; Evans and Clague 1994; Holm et al. 2004; Fischer et al. 2006; Kos et al. 2016) and the demise of the Late Pleistocene ice sheets (Gardner 1980; Abele 1997; Mercier et al. 2013). Indeed, exposure of glaciated rock-slopes may represent “one of the most significant geomorphological consequences of deglaciation in mountain environments” (Ballantyne 2002b, p. 1938). Proposed explanations for this association reflect glacial erosion, retreat and thinning (downwastage) that may precondition, prepare or trigger RSF activity over timescales of years to millennia (McColl and Draebing 2019). These mechanisms are briefly summarised below; readers are directed to McColl (2012) and Pánek and Klimeš (2016) for more detailed accounts.

Rock-slope failure factors

Controls on paraglacial rock slope (in)stability vary considerably with time, especially on glacial-interglacial timescales, and include the distribution and thermal regime of ice, glacial erosion, rockwall hydrological and mechanical conditions, and seismicity. Factors that precondition rock slopes for failure include geotechnical and topographic properties, and ultimately control the distributions, magnitudes and frequencies of failure. McColl and Draebing (2019) helpfully differentiate factors that prepare slopes, reducing slope stability to a critical state, from those that trigger final failure (Fig. 5.2). The former include progressive growth of fractures, and seismicity arising from the unloading of glacial and bedrock loads over century to millennial timescales. These reduce rock-mass strength (resistance) and/or increase the magnitude of potential triggers. Triggering factors include the propagation of fractures (and consequent rock fatigue) caused by hydrological and thermal effects that vary

on daily to seasonal timescales, but are superimposed on long-term climatic trends, as well as seismic shocks.

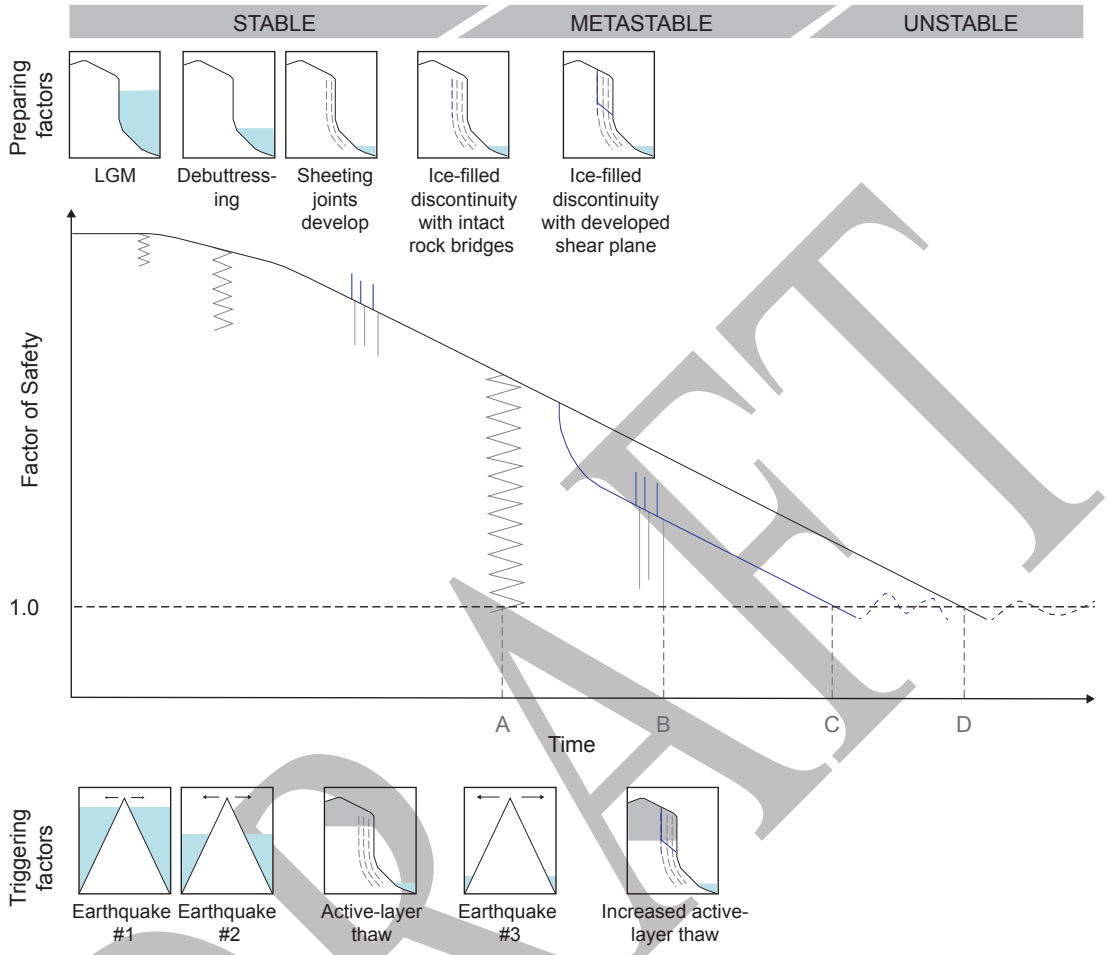

Fig. 5.2. A model for the reduction in stability of a rock-slope over time in response to changing internal and external factors that prepare slopes for failure and trigger final failure. Stability, expressed as the Factor of Safety, declines through time along different potential trajectories. Failure (a value below unity) occurs when resisting forces are exceeded by destabilising forces. New preparatory factors (depicted in the cartoons above) initiate more rapid reductions in stability as deglaciation and climate warming progress. Potential triggers are represented underneath the line and in the corresponding schematic cartoons below the main graph. A system-state change from rock-dominant state (black line) to an ice-dominant state (dark blue line) occurs when an ice-filled discontinuity with a continuous shear plane develops, and the system is more sensitive to failure. Letters A-D on the x-axis represent the breaching of external thresholds at A and B, and internal thresholds at C (sensitive rock state dominated by ice-filled fractures) and D (e.g. weathering-triggered). Source: McColl and Draebing 2019, Fig. 2.

The role that glaciation and deglaciation play in priming slopes for failure or triggering failures can therefore span timescales of years to millennia, sometimes initiating failure long

into subsequent interglacial periods (McColl 2012) and over multiple glacial cycles (Fig. 5.3; Grämiger et al. 2017, 2018; Hermanns et al. 2017b).

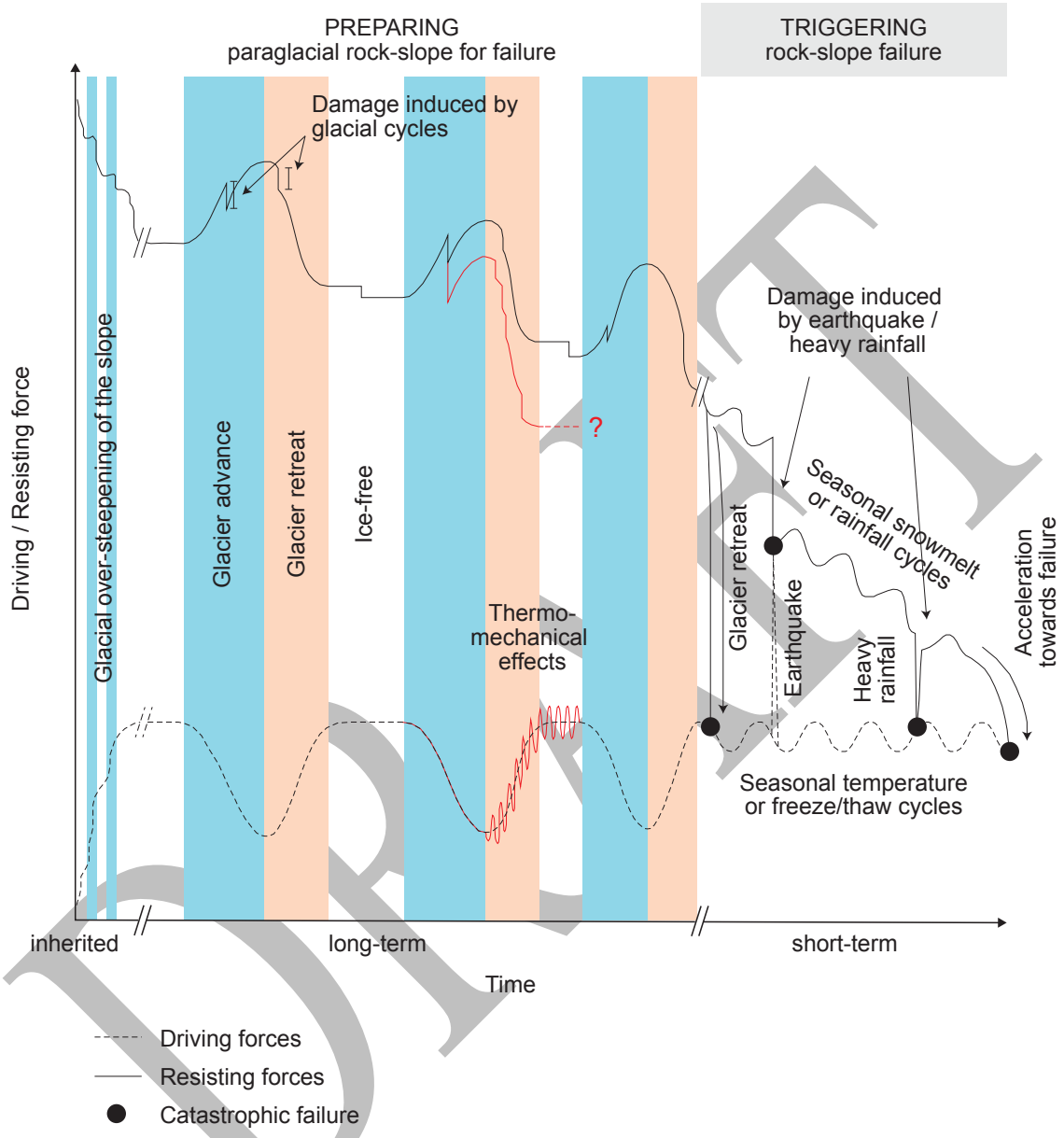

Fig. 5.3. Schematic representation of paraglacial preparation of a rock-slope until ultimate failure, with variation of driving and resisting forces during multiple glacial cycles. Incremental damage induced by glacier advance and retreat as purely mechanical loading and unloading (Grämiger *et al.* 2017), together with other preparatory factors during ice-free conditions reduces slope stability until a critical state is reached. A single small disturbance may ultimately trigger for catastrophic failure. Glacial cycles and other fatigue mechanisms (e.g. thermomechanical effects) may be more effective in preparing slopes for failure (red line). Source: Grämiger *et al.* 2018, Fig. 1a.

Prolonged glacial erosion can prime rock slopes for postglacial failure by steepening and lengthening slopes (which may increase overburden shear stresses behind the rock face), and unloading them of rock overburden (Radbruch-Hall 1978; Bovis 1982; Augustinus 1995a, b). Subsequent glacier retreat removes lateral ice support, exposes slopes to a new weathering regime, and enhances rock mass weakening initiated by unloading. Glacial debuttressing, often cited as a major driver of paraglacial rock-slope instability, may either trigger failure, or prepare a slope for failure at a later time (Holm et al. 2004; Cossart et al. 2008; McColl and Davies 2013; Kos et al. 2016; Grämiger et al. 2017). However, while it adds confinement to the slope stress field, over decadal and longer timescales glacier ice exhibits ductile behaviour, and so represents a weak buttress for glaciated valley walls. Stress redistribution and thermomechanical stress effects (so-called 'paraglacial thermal shock') accompanying glacier fluctuations may be significantly more effective in weakening bedrock than the purely mechanical effects of glacier loading and unloading alone (Grämiger et al. 2018). The fact that the timing of RSF activity appears to often lag deglaciation by several millennia (Ballantyne et al. 2014a, b; Ballantyne and Stone 2013) indicates that glacial debuttressing (as often described) is of limited importance in explaining long histories of paraglacial rock-slope adjustment.

Ice-loading of rock exerts high internal stresses, often causing elastic deformation of rock masses that is stored as residual strain energy (Wyrwoll 1977). During ice downwastage and unloading of glacially stressed rock, that energy is released, redistributing the orientation of principal stress fields within the rock, which may result in the development of a tensile stress zone behind the rock face (Ballantyne 2002b). As those surfaces are exposed, relaxation of tensile stresses causes lateral stress-release (rebound), joint network propagation and reduced cohesion, which may either lead to immediate or delayed RSF activity, depending on the dissipation of residual stresses (Wyrwoll 1977), as well as rock mass properties, valley geometry, and local environment.

Thus, rock fatigue is induced by both high, static overburden stresses enhanced by glacier erosion and downwastage, and a suite of cyclic stresses attributed to seismicity, thermal changes and fluctuations in water and ice loading in joints (McColl 2012; Krautblatter et al. 2013; Grämiger et al. 2017). Progressive strength degradation and the development of stress-release fractures may in part explain the timing and distribution of some postglacial rock slope failures (Ballantyne *et al*. 2014a).

Rock-slope failure responses

Steep rock-slopes can respond to the aforementioned stability changes in three ways (Ballantyne 2002b): catastrophic failure, deep-seated gravitational slope deformation, and rockfall.

Catastrophic failures are highly mobile movements of debris including major rockslides and rock avalanches, usually larger than 10^6 m^3, along a continuous failure plane. They involve substantial fragmentation of rock mass during runout and usually persist in the landscape (Hermanns and Longva 2012). Catastrophic failures during or soon after ice downwastage and retreat have been attributed to thinning and debuttressing of oversteepened glaciated rockwalls, permafrost degradation and isostatic seismic shock, while failure delayed (up to several millennia) after deglaciation (referred to as 'pre-failure endurance' by Ballantyne 2002b) may relate to long-term, progressive stress-release and strength degradation, or transient triggering mechanisms (Evans et al. 1989; Sigurdsson and Williams 1991; McColl 2012; Ballantyne and Stone 2013; Steiger et al. 2016; Rodríguez-Rodríguez 2018).

Paraglacial stress release has also been cited as a factor preparing slopes for rock-slope deformations (sackungen), whereby extremely slow flow (creep or sagging) causes mountain slope displacement without catastrophic runout of debris (Bovis 1990; Blair 1994; Agliardi et al. 2001). The landform signature associated with this mechanism includes prominent toe-slope bulging, antiscarps, ridge-top depressions, downthrown blocks and tension cracks, testifying to slow, subsurface deformation of the rock mass within unstable slopes (Jarman and Ballantyne 2002; Jarman 2006; Crosta et al. 2013; Pánek and Klimeš 2016). Locally, rock-slope deformation may represent a precursor to catastrophic failure (Holm et al. 2004; Hermanns et al. 2013a).

A third response of glacially-steepened rockwalls to deglaciation is initially rapid rockfall activity and talus accumulation below cliffs (Augustinus 1995a). On the basis of the large volumes of relict talus beneath rockwalls deglaciated in the Late Pleistocene, numerous authors have inferred that the rate of rockfall immediately after deglaciation greatly exceeded present (low) rates (Johnson 1984; Marion et al. 1995; Hinchliffe and Ballantyne 1999; Curry and Morris 2004). Disentangling paraglacial effects from periglacial forcing and rock

mechanical properties presents a challenge in evaluating destabilising factors for rockfall activity in formerly glaciated areas (Wilson 2009, 2017; Cossart et al. 2014).

Paraglacial rock-slope adjustment: assessment

Until recently, though, evaluation of these factors responsible for glacial conditioning of rock-slope activity has been impeded by a lack of regional-scale datasets on the spatio-temporal distribution of postglacial RSFs from tectonically inactive regions (Ballantyne *et al*. 2014a). In this context, a rapidly growing inventory of exposure-dated RSFs in the mountains of Norway presents a rich opportunity to characterise the timing of this activity and assess competing explanations for long- and short-term causes.

5.3 Setting and landscape development

Consideration of the nature and effects of paraglaciation at regional scales facilitates understanding of spatio-temporal dependencies and controlling parameters. Paraglacial rock-slope adjustment has been studied in western Norway (vest-Norge), comprising Møre og Romsdal, Sogn og Fjordane, Hordaland and Rogaland counties (Fig. 5.4). Relevant characteristics pertaining to the study area are summarised in this section.

Geology

Western Norway represents the uplifted surface of a tilted passive margin dominated by metamorphic rocks of Precambrian to Lower Palaeozoic age (Fig. 5.4c). The area consists mainly of Precambrian basement (Western Gneiss Region) in the north (Møre og Romsdal) and the western part of Sogn og Fjordane, with the SW-NE aligned Caledonian nappes (e.g. Lindås, Finse, Jotun nappes) underlying the central mountains (Tveten et al. 1998). There are also Devonian sedimentary basins along the coast between Nordfjord and Sognefjord. Bedrock is highly tectonized due to protracted, ductile and brittle tectonics acting since Precambrian times over the entire region (Gee and Sturt 1985). This has resulted in a high density of brittle and ductile structures and strong structural control of RSFs in the study area (Henderson and Saintot 2011; Saintot et al. 2011).

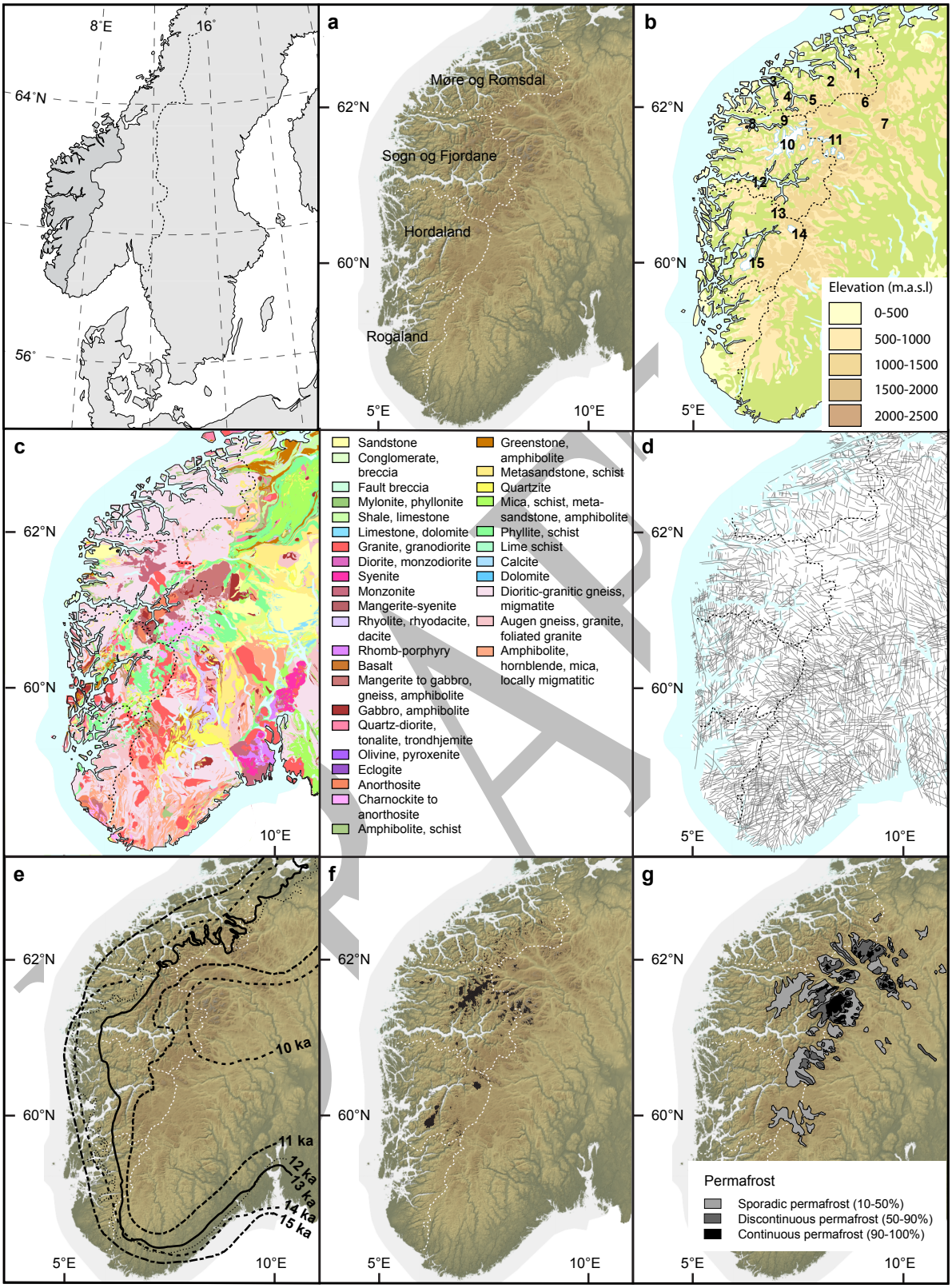

Fig. 5.4. Location and context of the study area in Norway: (a) the four counties of western Norway; (b) relief and selected localities referred to in the text: 1 Innerdalen, 2 Romsdalen, 3 Storfjord, 4 Årknes, 5 Tafjord, 6 Dovrefjell, 7 Rondane, 8 Nordfjord, 9 Loen, 10 Jostedalsbreen, 11 Jotunheimen, 12 Sognefjord, 13 Flåmsdalen, 14 Hardangerjøkulen, 15 Folgefonna; (c) geology and (d) faults (Geological Survey of Norway database: http://geo.ngu.no/kart/berggrunn); (e) pattern of Late Weichselian deglaciation of the

Scandinavian ice sheet across western Norway since 15 ka (Hughes *et al.* 2016); (f) current glacier extent (Andreassen and Winsvold 2012); and (g) modelled distribution of permafrost (Gisnås *et al.* 2016). Norwegian Mapping authority base map: https://www.geonorge.no/

Postglacial isostatic uplift rates at ~11 ka have been documented in the order of 50-500 mm yr^{-1} for Fennoscandia (Mørner 1979). Observed present-day uplift of western Norway is 2-3 mm yr^{-1} (Dehls et al. 2000a; Fjeldskaar et al. 2000), while debate surrounds the contribution of potential neotectonic processes. Generally, Norway has a low to intermediate seismic intensity (Fjeldskaar *et al*. 2000), though an area of earthquake activity is concentrated west of mid-Norway, related to a rifted passive continental margin (Bungum *et al*. 2005).

Quaternary glaciation

During Quaternary glacial cycles the landscape was inundated beneath the Scandinavian ice sheet and mountain ice caps on multiple occasions, causing repeated bedrock loading, unloading and isostatic rebound. A mean bedrock lowering of ~520 m has been calculated for central Norway (Dowdeswell et al. 2010), though vertical linear erosion along fault-controlled valleys amounted to 1500–2000 m (Mangerud et al. 2011).

The last (Weichselian) glaciation started at the end of the Eemian (MIS 5e), with the Scandinavian ice sheet reaching its last glacial maximum (LGM) extent at different sectors between ~27 and 21 ka (Mangerud et al. 2011; Olsen *et al*. 2013; Hughes et al. 2016). Mangerud (2004) considered that at its LGM the ice sheet covered almost all mountains in southern central Norway, though some mountains along the west coast fjords may have projected as nunataks.

Late Weichselian deglaciation commenced with the ice margin progressively withdrawing from its maximum limits, likely reaching the inner fjords of western Norway during the Bølling/Allerød interstadial, ~14.7 – 12.7 ka (Sollid and Sørbel 1979; Aarseth et al. 1997; Longva et al. 2009). However, ice sheet decay in western Norway appears to have been asynchronous from ~14-12 ka (Fig. 5.4e), with the ice front first retreating southwards from the coast in Møre og Romsdal (Hughes et al. 2016). Clearly, this ice retreat led to major thinning of the remaining ice sheet further inland, and progressive exposure of glaciated rockwalls. Deglaciation was interrupted during the Younger Dryas cold reversal (12.9–11.7 ka, Lohne et al. 2013), when significant ice thickening and readvances (several tens of

kilometres) occurred in most, but not all western sectors of the Scandinavian ice sheet. Locally, ice reached thickness of 800–1200 m in fjords that had been ice-free during the Allerød (Mangerud 2004). After 11.5 ka, however, ice retreat was rapid. Deglaciation of the main valleys around the Jostedalsbre and Jotunheimen massifs is likely to have occurred by ~9.7 ka (Rye et al. 1987; Karlén and Matthews 1992; Dahl *et al*. 2002).

Neoglaciation and present-day glaciation

During the early Holocene, numerous glacier variations in western Norway were driven by abrupt, short-term climate variations, including the so-called '8.2 ka event'. Syntheses of Holocene glacier variations (Nesje et al. 2008; Winkler, Chapter 3, this volume) indicate the disappearance of most Norwegian glaciers, including the Jostedalsbre ice cap (Nesje *et al*. 1991) on at least one occasion during the Early or Mid Holocene, in response to high summer temperatures and/or reduced winter precipitation. Glaciers were most contracted from ~6.6 to 6.0 ka (Nesje 2009), at the end of the Holocene Thermal Maximum (HTM).

Since then, Neoglacial fluctuations have characterized the Late Holocene, culminating in the 'Little Ice Age' glacier maximum of the early 18th century to the late 19th century (Nesje *et al*. 2008). Overall retreat was asynchronous, beginning between ~AD 1750 and the 1930s–40s, since when glaciers in western Norway have predominantly been retreating, most rapidly since 2000 (Nesje *et al*. 2008). Winsvold et al. (2014) calculate that glacier area declined by *c.* 11% during the last *c.* 30 years. Future predicted mean annual warming of 0.3–0.4 °C per decade in Scandinavia (Benestad 2005) is likely to cause unprecedented glacier retreat by AD 2100 (Nesje *et al*. 2008).

More than half of glacier spatial coverage is currently concentrated in Sogn og Fjordane (on and around Jostedalsbreen), with the remainder mostly in Hordaland (Folgefonna and Hardangerjøkulen) and Oppland (Jotunheimen) (Fig. 5.4f).

The latest glacier inventory in Norway (Andreassen and Winsvold 2012) indicates that there were 1252 glaciers in southern Norway (including Oppland) covering a total area of 1520 km^2. Average glacier size was ~0.97 km^2, reflecting the predominance of small valley glaciers, cirque glaciers and ice caps. Two ice caps account for 42% of glacierized area in

western Norway - Jostedalsbreen (474 km^2), the largest glacier in continental Europe, and Søndre Folgefonna (164 km^2).

Terrain and climate

Inland from the coast, the terrain of western Norway is dominated by the Scandes mountain chain, with 75% land area exceeding 300 m elevation and 35% above 1000 m elevation (Fig. 5.4b). The highest summit is Galdhøpiggen (2469 m a.s.l.). Glaciations have formed numerous rockwalls, mostly located in the mountainous interior and along the western coast where steep, over-deepened glacial troughs reach below sea level and form a network of fjords intruding inland for up to 200 km.

Topographically, most valley-side slopes have experienced a considerable degree of glacial erosion. Much of the landscape is characterized by high relief, especially in the western fjords, where alpine-type relief locally exceeds 2800 m. Elements of ancient paleic surfaces are preserved as more gentle, high-altitude plateaus above deeply incised valleys (Gjessing 1967; Etzelmüller *et al*. 2007).

The climate of western Norway exhibits significant variation between marine (Cfb) and subarctic or boreal (Dfc) types at the coast to tundra (ET) in high relief areas inland. Thus, mean annual precipitation and temperature values decline inland from >3500 mm and 6°C on the coast to >1000 mm and -4°C in more continental, montane areas inland (Hanssen-Bauer et al. 2017). Strong seasonal patterns are superimposed on these averages, with cyclonic precipitation occurring during autumn and winter, and intense snowmelt in spring and prolonged frost periods, which may increase the vulnerability of rock-slopes in western Norway (Blikra et al. 2006).

Mountain permafrost is recognized as an important factor for RSF activity in Norway (Blikra and Christiansen 2014) and is widespread in the high mountains. Its lower limit follows an altitudinal gradient in southern Norway from ~1600 m a.s.l. in the west to ~1300 m a.s.l. in the east (Gisnås et al. 2013; Steiger et al. 2016). In southern Norway, permafrost rockwalls are most common in the montane region surrounding inner Sognefjord and Jostedalsbreen, and Møre-Romsdal, as well as in the Hurrungane, Rondane and Dovre mountain areas (Fig. 5.4g). Hipp et al. (2014) described strong topographic aspect dependency of permafrost

occurrence of around 500–600 m in the Jotunheimen area. Modelling of predicted warming suggests continued rising of the lower limit for mountain permafrost to ~1800 m.a.s.l by the end of this century (Hanssen-Bauer *et al*. 2017).

5.4 RSFs in western Norway: processes and spatial distribution

Catastrophic failures of rock-slopes represent one of the most serious natural hazards in the glacially-oversteepened mountain and fjord landscapes of western Norway. In addition to their direct impacts, possible secondary effects of valley impoundment (Hermanns et al. 2013b) and displacement waves in fjords and lakes (Hermanns et al. 2006a; Harbitz et al. 2014) represent an especially high risk (Fig. 5.5). In the past century 175 lives were claimed by three RSF activity and secondary effects (Blikra et al. 2006; Oppikofer et al. 2016). A firm appreciation of the mechanics, frequency and chronology of these events are of major importance for hazard evaluation and for understanding the behaviour of unstable rock slopes under scenarios of future change.

This section identifies the main processes, spatial and temporal distribution of paraglacial rock-slope responses in western Norway. Emphasis is placed on the prehistoric record of large-scale (>0.1 M m^3) failure events, for which an extensive data inventory is emerging. Establishing these patterns can assist in the identification of local and regional controlling parameters.

5.4.1 Mechanisms of rock-slope failure

Forms of rock-slope adjustment in western Norway range from rock-slope deformations (sackungen), and translational slides of relatively intact bedrock, to fully disintegrated rock avalanches, and discrete rockfall activity. Assessing the significance of failure mechanisms is hampered, however, by inconsistent use of nomenclature. For example, terms such as megalandslide, rock avalanche, and catastrophic failure are often used synonymously.

Nonetheless, it is widely considered that large rock avalanches dominate in western Norway's steep, high relief troughs and fjords (Blikra et al. 2006). Longva et al. (2009) distinguished rock avalanche from rockfall deposits in terms of a minimal volume of 0.1 M m^3 for the former. Rock avalanches are typically characterized by high velocities and

significantly longer runout distances than for rockfalls (Hermanns and Longva 2012). Many rock avalanche deposits overlie deformed valley-fill sediments and are characterised by coarse debris cones and lobes supporting a chaotic surface topography of ridges, mounds and basins. Runout debris from valley-wall failures often extends >1 km, unless constrained by the opposing valley slope. Nearly all historical rock avalanche events are deemed to have followed active rock slope deformation, either shortly before or long in advance of failure (Hermanns et al. 2013a).

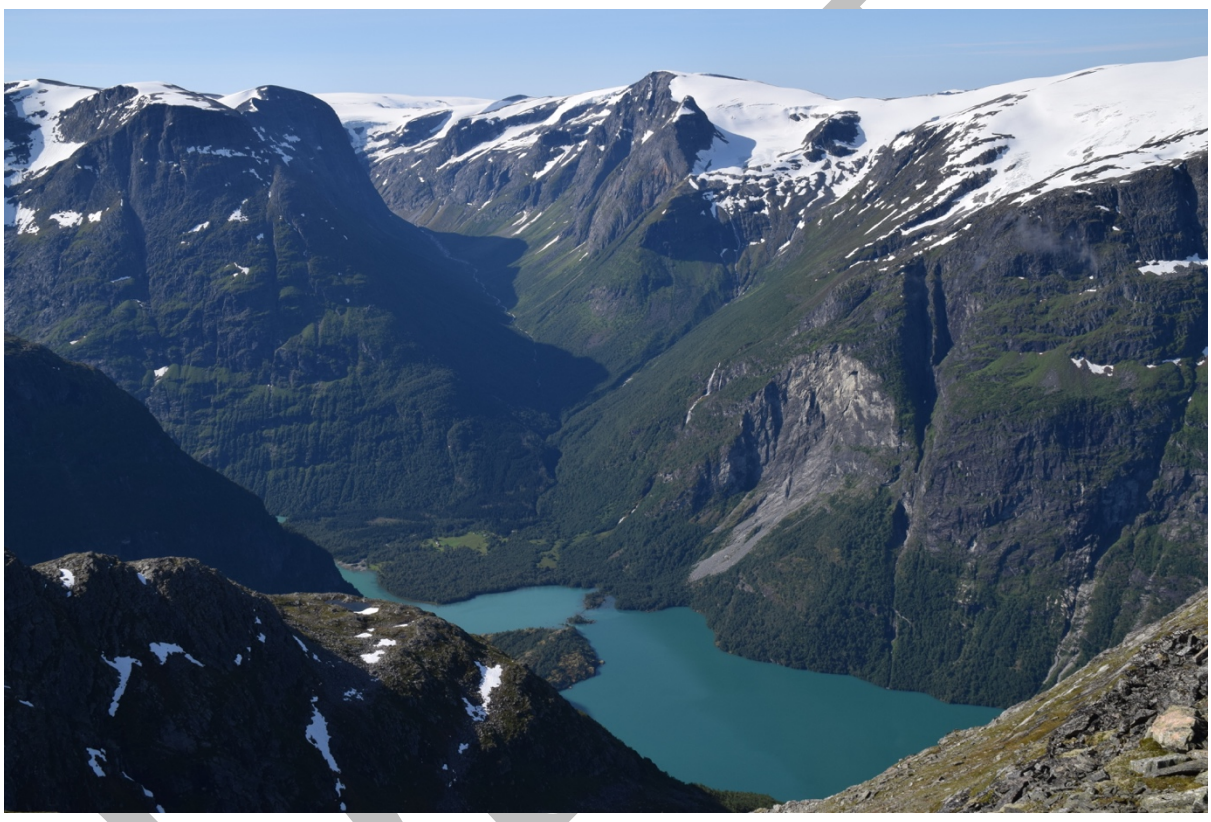

Fig. 5.5. Slide scar and rock avalanche debris below Ramnefjellet (1,779 m) at Loen, Sogn og Fjordane. The top of the scarp is 900 m above the level of the lake Lovatnet, and displays outward dipping joint sets and foliation in generally massive granitic gneisses. Seven rock avalanches occurred here between AD 1905-1950, with four failures from September-November, 1936. Tragically, subsequent displacement (tsunami) waves of 40.5 and 74 m height killed 61 people in 1905 and 73 people in 1936, respectively. The total volume of displaced rock was estimated to be >3.2 x 10^6 m^3 (Grimstad and Nesdal 1990). Local clustering of RSF events at Loen highlights the potential for the same slope to undergo repeat failure over short timescales. Photo: Paula Hilger.

Failures may frequently be initiated, however, as translational slides. Of 72 unstable rock-slopes mapped by Saintot et al. (2011) in western Norway, the majority (48) were defined as (translational) rockslides. Yet failure mechanisms are often complex and their forms composite. A promising approach for better understanding the deformation and failure

mechanisms of complex unstable rock-slopes appears to lie in the integration of detailed geological and monitoring data with structural and kinematic analysis and numerical modelling (e.g. Böhme et al. 2013; Booth et al. 2015; Oppikofer et al. 2017; Sandøy et al. 2017).

5.4.2 Slope-scale distribution of RSF activity

At the local scale, the balance between shear stresses and shearing resistance of a rock mass is determined by the highly variable interplay between mechanical, thermal and hydrological bedrock characteristics, as well as rock weathering processes (Messenzehl et al. 2017). These authors assert the relative contribution of geotechnical, topo-climatic, cryospheric and paraglacial properties is determined by a complex interaction with small-scale bedrock morphometry and overall valley topography. Intact rock strength, joint density and orientation relative to slope, bedrock roughness and morphometry constrain spatially-variable stress fields, while bedrock moisture, the presence of permafrost and segregation ice, strongly influence the effectiveness of weathering cycles.

The geological and topographic controls on rock-slope instability, including rock-slope morphometry, are clearly evident at the local scale in western Norway (Böhme et al. 2012, 2013). Gravitational slope deformation at Stampa (Sogn og Fjordane) is strongly controlled by inherited structures, such as pre-existing joint sets and the metamorphic foliation of the phyllites. These authors observed large open fractures or surface depressions developed along the main joint sets or a combination of two of them. Numerical modelling also supports structurally controlled failure, where discontinuities with a low strength dominate the rock mass behaviour.

Böhme et al. (2011) found that 79% of rock-slope instabilities in Sogn og Fjordane have developed either at convex breaks of slope (knick-points) that are interpreted to be of glacial origin (Holm *et al*. 2004), or at the unstable edges of high plateaux (Fig. 5.6). The authors' findings agree with geometric models of rock-slope failure in Norway (Braathen et al. 2004) that predict rockfall and topple failure at plateau edges and rocksliding at convex profile knickpoints. These findings also echo those drawn from modelling the controls on rockfall in the Swiss Alps (Messenzehl et al. 2017), where the vulnerability of permafrost rockwalls to

rockfall were linked to convex, steep terrain (>40°) and north-facing valley flanks, promoting surface moisture supply and subsurface lateral heat fluxes.

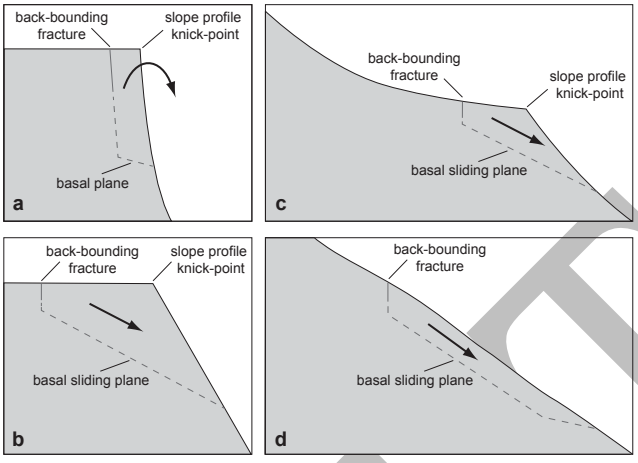

Fig. 5.6. Schematic representation of types of rock slope instabilities in western Norway based on pre-failure geomorphology. Rock slope instabilities in Sogn og Fjordane are located at unstable edges of plateau-like surfaces (a and b), and at knick-points of slopes (c) but are not situated directly on a steep slope with constant slope angle (d). Typical modes of movement are fall or topple for (a) and slide for (b)–(d). After Böhme *et al.* 2011, Fig. 9.

Finally, at the slope scale, the distribution of postglacial RSFs can be driven by different mechanisms at different points on a slope profile, and different sectors of a slope can be activated at different times (Leith et al. 2010a, b). In this way, different parts of a rock mass can reach a state of critical conditional stability at different points in time, causing some unstable slopes to collapse repeatedly while others fail in a single event (Hermanns et al. 2013a). Generally, RSF activity can increase the probability of future failures in the vicinity because of accelerated unloading along the rock slope (Hermanns, et al. 2006a).

5.4.3 Regional-scale distribution of RSF activity

One way to evaluate the influence of glacial conditioning on RSF activity has been to relate the location of failures at the basin scale to former glacier limits, and other possible influences such as topo-geometry, lithology, seismotectonics, permafrost degradation and freeze-thaw. The abundance of RSFs in glacially steepened and over-deepened valleys has been widely recognised. While spatial associations of long, steep, glacially-modified terrain and clustering of RSFs make a strong case for (de)glacial conditioning of slope instability, they alone fail to explain failure mechanisms or triggers (McColl 2012). They also fail to

explain sparsity of RSFs in are of favourable geology and structure - many processes can produce long, steep slopes, but not all long, steep slopes fail. Moreover, generic factors (such as debuttressing, deglaciation meltwater and freeze-thaw) apply to entire montane areas and fail to explain spatial clustering of RSFs (Jarman and Harrison, 2019).

Despite progress in understanding failure mechanics and controls at the process-scale, assessment of the relative importance of different controls within a complex synergetic interplay is still lacking, especially at larger scales, where complex and emergent system behaviour (Phillips 2003) may mean that different causes trigger RSF activity at different scales (Messenzehl et al. 2017).

In a study of RSFs in the Scottish Highlands, Jarman (2006) noted that although glaciation affected the entire montane area in the last glacial cycle, slope failures are unevenly distributed (65% are found in seven main clusters, with the rest widely scattered), for which previous glaciological, lithological and seismotectonic explanations failed to adequately explain any pattern. Areas with similar relief and lithology could display either many or few failures. Jarman (2006, 2009) and Ballantyne (2008) identified RSFs in areas that experienced maximum glacial overburden, such as narrow troughs and breaches associated with particularly constrained glacier flow, and areas of flow convergence (such as confluent glacial valleys). Moreover, they recognised rock-slope instability focused in over-deepened basins, where steepening of the lower valley-wall prolongs destabilization of mountain slopes. In a review of more than 1,000 RSFs in the British mountains, Jarman and Harrison (2019) hypothesised that concentrated bedrock erosion in glacial breaches might have generated sufficient rebound stress differentials between lower and upper slopes to provoke failure, though this proposal is unverified.

Historical records and geological studies of western Norway show a high concentration of both post-glacial gravitational slope failures and current rock-slope instabilities. As of 2015, systematic mapping in the three counties with most historic events (Sogn og Fjordane, Møre og Romsdal and Troms) had revealed 253 unstable rock slopes: 117 in Troms, 91 in Møre og Romsdal, 23 in Sogn og Fjordane and 13 in Rogaland (Devoli et al. 2011; Hermanns et al. 2013c; Oppikofer *et al*. 2013 2015).

The highest frequency of failures was found in the high-relief, inner fjord areas of Møre og Romsdal, and Sogn og Fjordane (Fig. 5.7), while they are comparatively sparse in Rogaland, Hordaland and Rondane (Oppland) (Blikra *et al*. 2002, 2006; Böhme et al. 2011; Henderson and Saintot 2011). Almost 200 individual events have been mapped in Møre og Romsdal, with the greatest number in the Romsdalen and Tafjord valleys (Blikra *et al*. 2002, 2006). In Romsdalen (home to Trollveggen, Europe's tallest vertical rockwall), more than 15 large rock avalanches cover almost the entire valley floor over a distance of 25 km, while in Tafjord, more than 10 rock avalanche deposits have been mapped in the fjord over a distance of less than 7 km (Blikra *et al*. 2006). Åknes, on Sunnylvsfjord (Møre og Romsdal) is regarded the most hazardous rockslide area in Norway. In the same county, two smaller groups of failures occur in outer coastal locations around Otrøya and Syvdsfjord. Many RSFs are also found on weak schist (phyllite) in Aurlandsfjord and Flåmsdalen (Sogn og Fjordane).

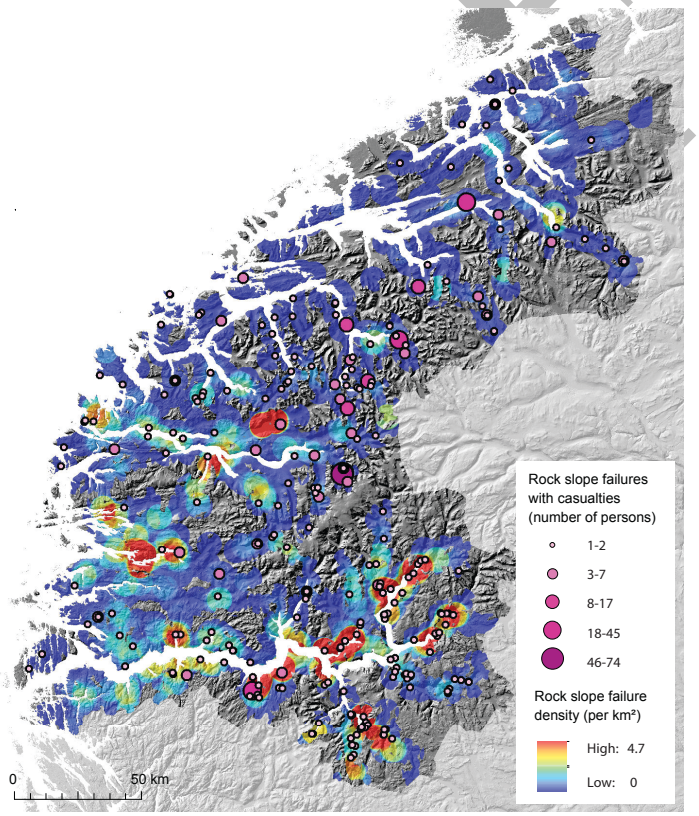

Fig. 5.7. Overview of historic RSF events and fatalities in Møre og Romsdal and Sogn og Fjordane counties, western Norway. RSF densities were calculated using a moving circular window with a 5 km radius. Source: Böhme 2014, Fig. 3.2.

Several studies have sought to quantify the spatial relations between RSF activity and geological and topographic parameters in western Norway (Böhme et al. 2011, 2014). These

authors highlighted a strong spatial association between the occurrence of rockfalls in Sogn og Fjordane and its Quaternary geology, tectono-stratigraphic position and density of geological lineaments.

Certainly, given the region's complex and protracted ductile and brittle tectonic history, it may be expected that inherited bedrock geology and structures have a strong influence on the spatial distribution of RSFs on high, steep (>35°) terrain. Lithology appears to be important in controlling the development of unstable rock masses, especially where failure planes coincide with the contact between hard, basement gneissic rocks and soft weathered mafic and ultramafic rocks (Böhme et al. 2011). Saintot *et al*. (2011) demonstrated that parameters favouring instability and failure in western Norway include (1) relatively weak foliated metamorphic rocks, such as phyllites, schists and foliated gneisses; (2) fjord- or valley-dipping foliation or steep, slope-parallel foliation; (3) folds; (4) Caledonian thrusts cutting the slope; and (5) regional brecciated (cataclastic) faults close to the slope. According to Henderson and Saintot (2011), large RSFs >3 x 10^6 m^3 only tend to develop in western Norway when all critical structures are present (valley-dipping foliation and a weakened plane at the base of the potentially unstable block, as well as existing lateral boundaries of the unstable block). These findings highlight the importance of pre-conditioning geological parameters, coupled with glacially-conditioned inheritance, for generating slope failure. Similarly, others have suggested that lithological and structural parameters are the most important long-term control on rock-avalanche clusters in the European Alps (Hermanns et al. 2006a; Ostermann and Sanders 2017), with seismicity and climatic factors often triggering failure.

While present seismic intensity in Norway is low to intermediate (Fjeldskaar et al. 2000), an offshore concentration of earthquake activity is clustered west of central Norway (Bungum *et al*. 2005), and some authors (Böhme et al. 2011; Henderson and Saintot 2011) speculate whether the regional clustering of rockslides in Møre og Romsdal may reflect greater postglacial seismic activity as well as steep, present-day uplift gradients (Fig. 5.8).

Permafrost thaw is widely recognised as an important factor for RSF activity due to melting of ice-bonds in cracks and weakening of tensile and compressive strength in rock masses (Murton et al. 2006; Krautblatter et al. 2012, 2013). Preliminary modelling of permafrost distribution in Norwegian rockwalls (Steiger et al. 2016) also promises to shed light on the

spatial clustering of RSFs. The results of this study imply that the highest spatial density of Norwegian rockwalls in permafrost follows an arc around the inner fjord areas of Møre og Romsdal, Sogn og Fjordane and the Rondane, associated with dissected, high-altitude paleic surfaces. The authors proposed that unstable rock slopes within the permafrost zone in southern Norway are mostly restricted to the large glacial valleys Romsdalen and Sunndalen in Møre og Romsdal, where valley-wall elevations commonly exceed 1500 m.a.s.l, and the area surrounding Jostedalsbreen (Sogn og Fjordane). By implication, thermal regime may be a further, important factor conditioning rock-slope instability in this region, at least for high elevation sites.

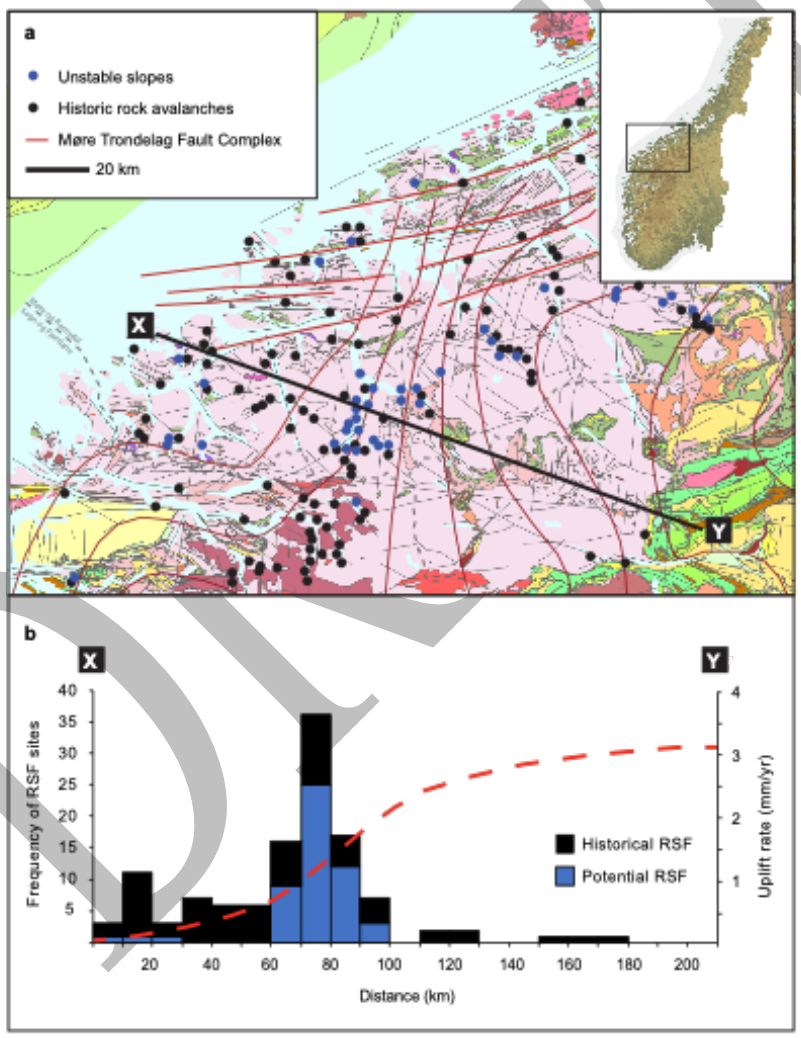

Fig. 5.8. Historical rock-slope failures and current rock-slope instabilities in Møre og Romsdal county, western Norway: (a) overview, showing current apparent uplift rates (mm/yr). Precambrian basement is shown in pink, Caledonian thrust sheets are in greens and yellows. Note clustering where uplift gradients are steep (Geological Survey of Norway database: http://geo.ngu.no/kart/berggrunn). (b) frequency histograms of RSF localities relative to uplift pattern (Vestøl, 2006; Olesen *et al.*, 2013). Profile X-Y includes landslides within 60 km of the profile. (Source: Henderson and Saintot 2011, Fig. 1).

In their attempt to identify and quantify regional-scale controls (topo-climatic, cryospheric, paraglacial or/and rock mechanical properties) on rockfall activity in the Swiss Alps, Messenzehl *et al*. (2017) recognized permafrost distribution as the major control on the spatial distribution of rockfalls. The authors attributed clustering of rockfall source areas within a low-radiation altitudinal belt at 2900–3300 m a.s.l. to rock weathering via seasonal growth of segregation ice in shallow permafrost. Analysis of 90+ small RSFs in Jotunheimen lends further support to this view. Using change detection and discreet Meyer wavelet analysis, combined with permafrost depth models, Matthews et al. (2018) identified a strong correlation between the spatial distribution of small ($<10^3$ m^3) RSFs and the aspect-dependent lower altitudinal limit of mountain permafrost in rockwalls.

5.5 Temporal pattern of RSF activity

Analysing the temporal pattern of slope failures is another means of assessing the influence of glaciation on rock-slope stability (McColl 2012; Ballantyne and Stone 2013; Ballantyne et al. 2014a). Timing datasets enable assessment of the random or clustered nature of landslide distributions, and comparison of these clusters with the timing of other events, for example, glacier retreat, climatic events, or seismicity, has been crucial in understanding the causes of enhanced rock-slope adjustment (McColl 2012).

5.5.1 Timing of prehistoric RSF activity

Former RSF datasets represent important archives, though detailed comparisons should proceed with caution, given that they represent different morphological settings with varying levels of chronostratigraphic resolution. Further, while aided by recent advances in absolute dating techniques, reconstructing the timing and causes of prehistoric RSF activity invariably represents a general approximation of a fragmentary record. The preservation of rock-slope debris is generally limited to terrain exposed since the last glaciation, though dating control may be further complicated where failure or deformation has been intermittently active over the course of multiple glacial cycles (Tibaldi et al. 2004), or where debris or unstable surfaces have been preserved under cold-based ice (Matthews et al. 2013; Hermanns et al. 2017b). Where clear stratigraphic sequences are unavailable, reliance on exposure dating of surface deposits may over-represent younger events if they overlie older deposits. Elsewhere, runout debris may have dammed valleys, prompted local aggradation and been buried (Dadson and

Church 2005), fallen into a fjord or lake and lack an onshore record (Hermanns and Longva 2012), or been recycled or removed by subsequent fluvial or glacial transport (Ballantyne 2013). Moreover, the number of supraglacial RSFs is likely under-represented in sediment records, as those deposits are reworked and can be difficult to distinguish from moraine deposits (Hermanns et al. 2017a). Coherent rockslides may lack good exposures for dating, and the most accessible RSF debris may result from secondary activity (Jarman and Harrison 2019). Finally, triggering events and causes of analogous historic failures are rarely observed, and often inferred (McColl 2012).

Large-scale failures

Notwithstanding these issues and caveats, recent years have seen a fruitful flourishing of research directed at the prehistoric evidence for rock-slope adjustment in western Norway (Blikra *et al*. 2002, 2006; Bøe *et al*. 2004; Aa et al. 2007; Fenton et al. 2011; Longva et al. 2009; Hermanns *et al*. 2017a). Assisted by geophysical, geodetic, geotechnical and geochronological advances, a programme of mapping terrestrial sites and surveying and coring Norwegian fjords has yielded a record of frequent, large-scale RSFs throughout the prehistoric period.

The general opinion of early attempts to date postglacial rock-slope activity in western Norway (and beyond) was that most failures occurred shortly after deglaciation at the end of the Pleistocene, when glacio-isostatic uplift was most rapid, and pressure-release likely promoted sudden unloading in the steepened and over-deepened alpine terrain, coupled with a high discharge of meltwater into bedrock fractures. Glacially-conditioned rock mass fatigue in western Norway was recognised by Peulvast (1985), who attributed tensile stress conditions at the toe of glacial troughs in Sogn og Fjordane to increased overburden shear stresses associated with glacial erosion (*cf.* Augustinus 1995b; Jarman 2006, 2009). Further, now-largely dormant or inactive, widespread gravitational structures are considered to have been generated during the Late Pleistocene, in glacially-conditioned rockwalls (Saintot et al. 2011). The latter study highlights a strong association between rock-slope weakening, steep relief and the density of brittle structures that most recently developed during regional deglaciation.

Certainly, there appears to be support for a peak in rock-slope activity during or shortly after regional deglaciation in Norway. In Troms county, in the north of the country, eight dated large, RSFs occurred in a period shortly after the last (Weichselian) glaciation, ~10.5-11.5 ka, and only few large failures are recorded there in historical times (Blikra et al. 2006). In western Norway, a similar temporal pattern seemingly exists in the outer, coastal area of Møre og Romsdal, where rock avalanches probably occurred shortly after deglaciation: at ~15-14 ka on Øtrefjellet, >11.5 ka in Ørsta, and at <11.5 ka in Syvdsfjord (Blikra et al. 2002).

Fig. 5.9. Vegetated debris cones below a triangular failure scarp on the south flank of Alstadfjellet (1,450 m), in Valldalen, Møre og Romsdal. Cosmogenic nuclide (^{10}Be) ages averaging 9.3±1.0 ka were obtained for the slope-foot rock-avalanche deposits (Hermanns *et al.* 2017a), approximately 5 ka after deglaciation at this locality. Photo: Peter Wilson.

More recent research, however, has revealed a more complicated picture, especially in the inner fjord areas of western Norway. In addition to enhanced Late Pleistocene rock-slope adjustment, many catastrophic RSFs are now known to have occurred throughout the Holocene (Blikra et al. 2002, 2006), with a possible Holocene peak at ~3 ka, as well as during historical times (Fig. 5.9). A rock avalanche in Oldedalen (Nesje 2002), for example, occurred some 6000 years ago, coincident with the age of the formation of the Jostedalsbreen

ice cap (Nesje et al. 2001). Nesje (2002) speculated whether failure may have been associated with renewed local glaciation, via changes in rockwall joint-water pressures.

Blikra et al. (2002) interpreted seismic stratigraphy in Tafjord as recording individual events throughout the Holocene, with increased frequencies during the Late Holocene. Similarly, data from Aurlandsfjord and Flåmsdalen in Sogn og Fjordane suggest that RSF activity in the phyllite area is related to two stages, one shortly after deglaciation at ~11-10 ka and a smaller event at ~3 ka (Blikra et al. 2002).

Schleier *et al*. (2015) also found evidence for two episodes of RSF activity in Innerdalen (Møre og Romsdal), in the form of a rock avalanche falling onto the surface of a downwasting glacier at ~14 ka, followed by a Holocene event at ~8 ka. In inner Nordfjord (Sogn og Fjordane), a multi-stage pattern is evident, where 11 large rock avalanches occurred during most of the Holocene until ~3.2 ka (Aa et al. 2007; Hermanns et al. 2017a). Four events were dated to within 2 ka of deglaciation at ~13.5 ka, while a further 6 rock avalanches occurred between ~7.1 and 3.2 ka, at an average frequency of ~1 per 700 years. Finally, in Romsdal (Møre og Romsdal), Hilger et al. (2018) report exposure ages for three large RSFs between 12 and 10 ka, during a phase of paraglacial relaxation, as well as a period of between three and six catastrophic rock avalanche events that cluster at 4.5-5.5 ka.

A large dataset from inner Storfjord and its tributaries in Møre og Romsdal is especially intriguing in elucidating the temporal dynamics of rock-slope adjustment in this area. Based on a ^{14}C-dated sediment core and seismic stratigraphy, Longva et al. (2009) tentatively assigned ages to 108 rock avalanche deposits mapped on the floors of Storfjord, Nordalsfjord, Sunnylvsfjord, Geirangerfjord and Tafjord. Analysis of the Storfjord dataset in this relative chronostratigraphy suggested a rapid response and high frequency of rock avalanching following deglaciation, followed by a broadly constant frequency over the past 9 ka. 25 events (23% of the total number) deposited 89% of the total fjord rock avalanche volume (587 million m^3) during deglaciation (~14-11.5 ka), with five large events contributing 79% of the total debris volume. One-third of the Holocene events delivered half the total Holocene rock avalanche volume (65 million m^3) within 1,000 years of final deglaciation. The authors suggested this high frequency may reflect frost activity, permafrost thaw, exfoliation and strong earthquakes associated with rapid isostatic rebound. After a period of high rock-slope adjustment during Younger Dryas and Preboreal times (~13-9 ka), the remainder of the

Holocene at Storfjord appears to have been characterised by a generally even distribution of smaller rock avalanches, averaging 5-8 events per 1,000 years for the whole Storfjord system. Given the likely under-representation of prehistoric events preserved in the geological record, these figures should probably be considered minimal.

Exposure ages of a further 22 rock avalanches in western Norway were compiled by Hermanns et al. (2017a), who interpret their asynchronous temporal distribution of failures as primarily tracking the progressive decay of the Weichselian ice sheet. Half of the dated events in their inventory occurred within the first millennium of ice retreat. A further five events (22%) occurred during the Holocene Thermal Maximum (~8-5 ka), a period characterized by the warmest Holocene temperatures in Norway (Nesje 2009; Lilleøren *et al*. 2012). Whether or not this signifies an association with climate cannot be concluded on the basis of this small dataset. Four remaining events (20%) are relatively evenly distributed throughout the rest of the Holocene. These findings are in accordance with detailed analyses of rock-avalanche deposits in Storfjord that show that 51 out of 109 rock avalanches occurred within three millennia following deglaciation, and that more than 80% of rock avalanche debris was deposited in the fjord in the first millennia after deglaciation (Böhme *et al*. 2015).

RSF activity is frequently preceded by a period of accelerated slope deformation especially under non-seismic conditions (Eisbacher and Clague 1984). Dating of six sliding planes was undertaken for unstable rock slopes in Møre og Romsdal and Sogn og Fjordane by Hermanns et al. (2012, 2013b, 2017b) to determine the timing of initiation of deformation and long-term slip rates. At Oppstadhornet (Otrøya) and Skjeringahaugane (Lustrafjord), sliding has taken place at a constant rate since deformation initiated during deglaciation at ~14.2 and 10 ka, respectively. Preliminary interpretation of Storehornet (Homindal) suggests a period of deformation shortly after deglaciation was followed much later by a rock avalanche event during the Late Holocene. Delayed deformation is also evident at Ivasnasen (Sunndalen), where simultaneous sliding and failure (rock avalanches) were dated to ~3.5 ka (Oppikofer et al. 2017).

Finally, it is relevant to briefly mention the fjord and lake record of colluvial mass movements in western Norway, which suggests increased frequencies of turbidites, floods, debris flow and snow avalanche activity immediately after deglaciation, with episodic enhanced activity in the Late Holocene (Blikra and Nemec 1993; Bøe et al. 2002, 2003, 2004;

Lepland et al. 2002; Bellwald et al. 2016). These latter pulses of soft sediment reworking have been primarily attributed to inwashing during regional climatic irregularities, for example at 5.6-5.3 ka and especially at 3.2-2.8 ka, though seismic activity is considered an important regional trigger for increased mass movements at ~11.7-11.0 and 2.2-2.0 ka.

In a recent compilation of sediment cores and seismic profiles from 22 fjords and lakes in Sogn og Fjordane and Mør og Romsdal, Bellwald et al. (2019) dated 125 turbidites and mass movement deposits, and propose temporal clustering of increased mass movement activity for two periods in the Early Holocene (11.0–9.7 and 8.3–7.8 ka), followed by quiescence, and renewed mass movement activity since ~4.2 ka. Notwithstanding limited chronological control, the authors suggested broad, regional correspondence in the timing of episodic enhanced mass movement, offshore slides and rock avalanche activity, and proposed that seismic activity was the most plausible regional trigger, driven at least during the Early Holocene by glacio-isostatic rebound.

Small-scale failures and rockfalls

While much prior research has focused on catastrophic RSFs in Norway, less attention has been directed to small ($<10^3$ m^3, Matthews et al. 2018) features in the context of assessing the significance of paraglacial RSF activity. This is important, given that the occurrence, magnitude and frequency of RSFs are influenced by a host of geological, topographic and climatic factors. Small RSFs are generally considered to respond to deglaciation over a shorter period of time than large RSFs (Ballantyne 2002a). Improved understanding of these controls on RSF occurrence requires a consideration of RSF magnitude, and is essential for accurate modelling of future, climate-driven RSF activity (Gariano and Guzzetti 2016).

In the largest study of its kind, Matthews et al. (2018) applied Schmidt hammer exposure-age dating (SHD) to construct a detailed regional chronology of the frequency and magnitude of 92 small RSFs in Jotunheimen. The authors failed to detect evidence for a strong activity peak immediately after deglaciation at ~10 ka, and attributed this to considerable downwastage of the Late Weichselian ice sheet by this time (Mangerud *et al*. 2011; Hughes *et al*. 2016), which may have reduced the scale of paraglacial effects on subsequent RSF activity. Using a weighted age–frequency distribution and probability density function analysis, they indicated four 10^2-10^3 year periods of enhanced, small RSF frequency (at ~8.9,

7.3, 5.9 and 4.5 ka). Maximum activity was reached at ~4.5 ka. Since then, the incidence of small RSFs in this region appears to have declined significantly. Matthews et al. (2018) interpret the timing of peak RSF frequency (and its lagging the Holocene Thermal Maximum by ~2 ka) as primarily a response to long-term changes in permafrost depth during episodes of relatively warm climate and transition to a seasonal-freezing climatic regime.

Similarly, Marr et al. (2019) applied SHD to five small RSFs in Opplendskedalen (Møre og Romsdal), which was deglaciated at ~11.5 ka. Their results show that three features stabilized during the Holocene Thermal Maximum and do not support the hypothesis that RSF activity predominately occurs shortly after local deglaciation. While assuming that these small RSFs likely reflect glacially-conditioned, long-term stress-release (in part), the authors identified climatic factors related to warming (e.g. permafrost degradation, snowmelt and increased joint-water pressure) as triggering mechanisms. While based on a very small sample size, the wider representativeness of their conclusions appears to be supported by Matthews et al., (2018).

Finally, and notwithstanding the difficulty of distentangling the effects of periglacial conditions and intrinsic paraglacial rockwall instability, the spatio-temporal distribution of rockfall talus-derived landforms (protalus rock glaciers and protalus/pronival ramparts) may also shed light on the occurrence, magnitude and frequency of small RSFs. SHD of three relict rock glaciers in Ottadalen (Oppland), north of the Jotunheim massif yielded SHD ages of ~11-9 ka (Matthews et al. 2013). These may represent paraglacial landforms that formed in response to enhanced rockfall during early Holocene deglaciation, though alternatively, they may be much older features that were preserved beneath cold-based ice.

Similarly, dating of five relict protalus ramparts and rock glaciers in the Romsdalsalpane mountains (Møre og Romsdal) and at Nystølsnovi (Sogn og Fjordane) yielded SHD ages of ~15-8 ka (Matthews and Wilson 2015; Matthews et al. 2017). These data were interpreted as suggesting these rockfall-derived landforms accumulated over a period of ~6 ka between regional deglaciation and the end of the Younger Dryas, when glacial debuttressing and permafrost degradation enhanced the release of rock debris from cliffs. Matthews et al. (2017) considered at least two of the rock glaciers to be primarily paraglacial landforms, at least in terms of debris supply. A protalus rampart in Opplendskedalen that yielded a SHD age of 5.6 ka was regarded by Marr et al. (2019) to have initially formed after deglaciation

and added to during the Early Holocene by rock debris supplied from a rockwall weakened by permafrost degradation.

5.5.2 Timing of historic RSF activity

The historical record of failure of rock-slopes, including rock avalanches and large rock falls in western Norway has been collected from historical archives (Furseth 2006), and modern activity (Fig. 5.10) is registered in databases maintained by the Geological Survey of Norway (NVE 2018).

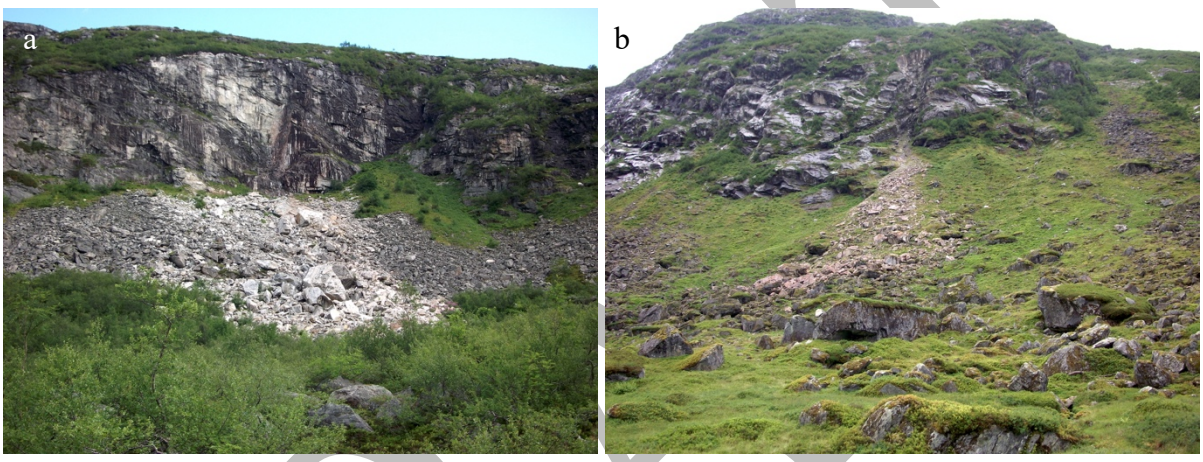

Fig. 5.10. Examples of small- to moderately-sized modern RSFs in western Norway: (a) a rockfall occurred that about AD 2005 on the south-facing slope of lower Langfjelldalen (Valldalen, Møre og Romsdal), at an altitude of 900 m; (b) the Nystølsnovi RSF (Langedalen/Austerdalen area of Jostedalsbreen) occurred in AD 1994. Photos: John Matthews.

Large rock avalanches are known to have caused a series of catastrophes throughout the historical period in western Norway, including at Loen in 1905 and 1936 (Fig. 5.5) and Tafjord in 1934 (3 M m^3), in which altogether 175 people were killed by displacement waves (Furseth 2006). The frequency and chronology of such events are of major importance for hazard evaluation and for understanding the behaviour of unstable rock slopes (Aa et al. 2007).

Rockfall activity in Norway reportedly increased during the 'Little Ice Age' (notably between the years AD 1650 and 1760), a phenomenon attributed to the increased frequency of extreme rainstorm events at that time (Grove 1972). However, there is little evidence for an increase in larger RSFs associated with post-'Little Ice Age' glacier retreat in mainland Norway

(Laute and Beylich 2013). The absence of a strong post-'Little Ice Age' rock-slope response may simply reflect significant lagging of bedrock permafrost thaw behind air temperature warming (R. Hermanns 2018, pers. comm.). Alternative explanations include the extremely limited and brief loading and unloading of rock-slopes by 'Little Ice Age' glaciers, combined with low rates of seismotectonic activity. The relative paucity of RSFs associated with 'Little Ice Age' ice retreat has been recognised elsewhere (e.g. Evans and Clague 1994; Jaboyedoff *et al*. 2012; Grämiger et al. 2018).

Both frequency and magnitude of historical RSF activity should be considered in temporal context. Extensive historical records of deadly or damaging RSF events in Norway during the past few centuries can give an impression of high levels of activity, though few accounts detail the volumes of failed rock. Based on historical records over the past 400 years, a frequency of 2-6 rock avalanches per century has been cited as an historical average for all Norway (Furseth 2006; Blikra et al. 2006). These historic rates appear to approximate Holocene averages, at least for several specific, active sites.

The Mannen area in lower Romsdalen, for example, is one such locality, where more than 30 historical RSF events were documented in the valley (NVE 2018), though these are primarily small (<100 m^3) rockfall events. Blikra et al. (2016) suggested a present-day recurrence interval in Romsdalen of <100 year for a 0.15 M m^3 failure, while the recurrence of a 2–4 M m^3 volume was estimated to be 100–1000 years. These present-day averages accord with dated records of 3-6 large rock avalanches within 1,000 years at Mannen, 4.5-5.5 ka (Hilger et al. 2018). A similar average rock avalanche frequency of 6-10 events per 1000 years was estimated for the last 9,000 years in Innerdalen and Storfjord (Aa *et al*. 2007; Longva et al. 2009). Low recurrence intervals for RSF activity imply post-failure rock-slope relaxation on decadal timescales (Schleier et al. 2017; *cf.* Hermanns et al. 2006a; Crosta et al. 2017). Sudden stress-release due to failure may cause weakening of the rock slope via reorganisation of the rockwall stress field (Hermanns et al. 2006b).

Several rockwalls in western Norway are known to have experienced multiple failures in recent years (Fig. 5.5). The Loen site (inland Sogn og Fjordane), for instance, failed repeatedly within a few decades in the early 20th century (Hermanns *et al*. 2006a). This observation raises questions for the interpretation of overlapping age ranges for prehistoric

failures at the same site, and whether such data represent one event or multiple failures from the same slope.

5.5.3 Causes and triggers of rock-slope failure: synthesis

The occurrence of RSFs of varying magnitude in western Norway's mountains reflects preconditioning and triggering by a wide range of environmental factors whose relative importance are likely scale-dependent. These factors include paraglacial stress release and fracture propagation due to unloading, debuttressing, palaeoseismicity, permafrost degradation and other climatic triggers (Ballantyne et al. 2014a).

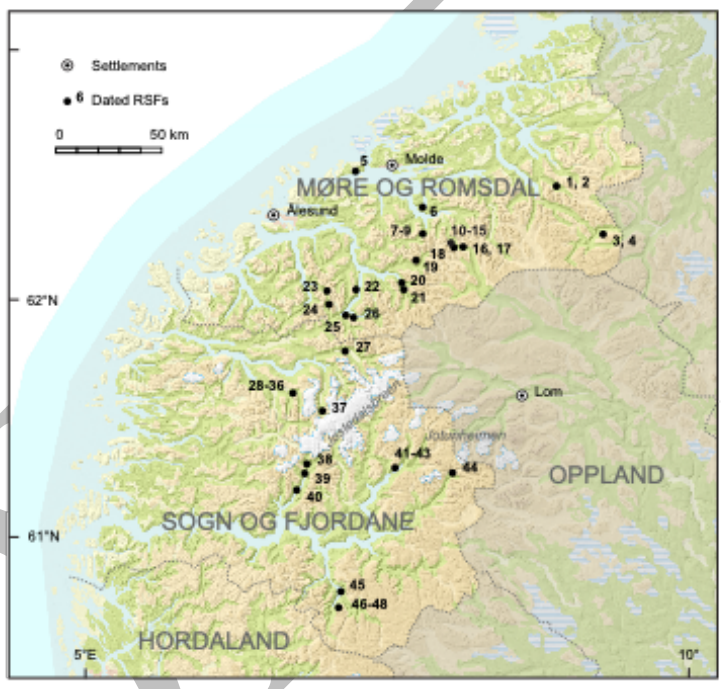

Fig. 5.11. Location of 49 moderate to large (>10^3 m^3) prehistoric RSFs in western Norway (numbering as in Table 5.1). Norwegian Mapping authority base map: https://www.geonorge.no/

This section seeks to characterize the timing of postglacial RSFs in western Norway and evaluates the significance of these factors. A preliminary analysis of the prehistoric RSF age inventories is presented, and timing data for 49 prehistoric RSFs are summarised in Table 5.1. Fig. 5.11 identifies the location of the sites. This work focuses on moderate to large (>10^3 m^3) RSF events with absolute dating control. Accordingly, records of colluvial mass movements are omitted from this preliminary investigation, and two important, large databases of Norwegian RSFs were also excluded - the Storfjord relative chronostratigraphic

Table 5.1 Collated timing data for 49 moderate to large (>10^3 m^3) prehistoric RSFs in western Norway, showing their main characteristics and estimated lag-time following glacier retreat.

RSF #	Location		Lithology	Type[1]	Volume (10^6 m^3)[2]	^{14}C age		Calibrated age		Method[3]	Lag ka[5]	Reference
						ka BP	Error 1σ	ka BP	Error 1σ			
	Møre og Romsdal											
1	Innerdalen (A-E)	Innerdalen	gneiss	RA	12			14.1	0.4	^{10}Be	<1	Schleier *et al.* (2015)
2	Innerdalen (F)	Innerdalen	gneiss	RA	22.5			7.97	0.94	^{10}Be	3.5	Schleier *et al.* (2015)
3	Ivasnasen (IF1)	Sunndalen	gneiss	RS/RA	5.4			13.0		STR	0	Oppikofer *et al.*, 2017
4	Ivasnasen (IF2)	Sunndalen	gneiss	RS/RA	1.6			3.3	0.1	^{10}Be (4)	9.0	Oppikofer *et al.*, 2017
5	Oppstadhornet	Otrøya	gneiss	DSGSD	10			15.4	1.2	^{10}Be	<1	Hermanns *et al.* (2013b)
6	Gråura	Romsdalsfjord	gneiss	RA				14.1	1.9	^{10}Be	1.0	Hermanns *et al.* (2017a)
7	Innfjorddalen (A1)	Innfjorddalen	gneiss	RA	20.6			14.3	1.4	^{10}Be	1.0	Schleier *et al.* (2017)
8	Innfjorddalen (C)	Innfjorddalen	gneiss	RA	6.3			8.79	0.94	^{10}Be	6.5	Schleier *et al.* (2017)
9	Innfjorddalen (D)	Innfjorddalen	gneiss	RA	0.4			1.03	0.38	^{10}Be	14.0	Schleier *et al.* (2017)
10	Mannen 1	Romsdalen	gneiss	RA				11.25	0.75	STR	0.4	Hilger *et al.* (2018)
11	Mannen 2	Romsdalen	gneiss	RA				9.39	0.3	^{10}Be	2.3	Hilger *et al.* (2018)
12	Mannen 3	Romsdalen	gneiss	RA				10.0	0.5	STR	1.7	Hilger *et al.* (2018)
13	Mannen 4	Romsdalen	gneiss	RA				4.93	0.09	^{10}Be	6.8	Hilger *et al.* (2018)
14	Mannen 5	Romsdalen	gneiss	RA				4.96	0.15	^{10}Be	6.7	Hilger *et al.* (2018)
15	Mannen 6	Romsdalen	gneiss	RA				4.95	0.1	^{10}Be	6.8	Hilger *et al.* (2018)
16	Skiri (1)	Romsdalen	gneiss	RA				11.7	1.3	^{10}Be	1.0	Hermanns *et al.* (2017a)
17	Skiri (2)	Romsdalen	gneiss	RA				11.0	1.3	^{10}Be	1.0	Hermanns *et al.* (2017a)
18	Svarttinden	Romsdalen	gneiss	RA				8.7	1.1	^{10}Be	3.0	Hermanns *et al.* (2017a)
19	Alstadfjellet	Valldalen	gneiss	RA				9.3	1.0	^{10}Be	5.0	Hermanns *et al.* (2017a)
20	Kallen	Tafjord	gneiss	RA				11.4	2.1	^{10}Be	1.0	Hermanns *et al.* (2017a)
21	Onilsavatnet	Tafjord	gneiss	RA	200			11.4	0.21	^{10}Be	1.1	Hermanns *et al.* (2009)
22	Blåhornet	Sunnylvsfjord	gneiss	RA	0.009			2.11	0.31	^{10}Be	9.9	Böhme *et al.* (2015)
23	Norangsdalen (Skylstad)	Sunnmøre	gneiss	RA				6.0	0.7	SHD	7.0	Nesje *et al.* (1994)
24	Norangsdalen (Uraseter)	Sunnmøre	gneiss	RA				4.2	0.8	SHD	9.0	Nesje *et al.* (1994)
25	Nakkaneset	Geirangerfjord	gneiss	RA				7.25	1.14	^{10}Be (4)	4.8	Böhme *et al.* (2015)

26	Nokkenibba	Geirangerfjord	gneiss	RA				7.06	1.25	^{10}Be (4)	4.9	Böhme *et al*. (2015)
	Sogn og Fjordane											
27	Erdalen	Erdalen	gneiss	RS		8.81	0.13	9.862	0.18	^{14}C	0.0	Hansen *et al*., 2009
28	Vora (a)	Myklebustdalen	gneiss	RA	80			12.9	1.9	^{10}Be	1.0	Hermanns *et al*. (2017a)
29	Vora (b)	Myklebustdalen	gneiss	RA				12.1	1.3	^{10}Be	1.0	Hermanns *et al*. (2017a)
30	Vora (c)	Myklebustdalen	gneiss	RA				9.49	0.5	SHD	2.0	Aa *et al.* (2007)
31	Vora (d)	Myklebustdalen	gneiss	RA				10.8	1.4	^{10}Be	1.0	Hermanns *et al*. (2017a)
32	Vora (Grisemyra B)	Myklebustdalen	gneiss	RA		6.2	0.04	7.09	0.08	^{14}C	5.0	Aa *et al.* (2007)
33	Vora (Grisemyra D)	Myklebustdalen	gneiss	RA		5.51	0.04	6.39	0.06	^{14}C	5.5	Aa *et al.* (2007)
34	Vora (Grisemyra F)	Myklebustdalen	gneiss	RA		5.065	0.035	5.82	0.07	^{14}C	6.0	Aa *et al.* (2007)
35	Vora (Grisemyra J)	Myklebustdalen	gneiss	RA		4.585	0.035	5.27	0.18	^{14}C	6.5	Aa *et al.* (2007)
36	Vora (Grisemyra O)	Myklebustdalen	gneiss	RA		4.47	0.05	5.13	0.15	^{14}C	8.5	Aa *et al.* (2007)
37	Oldedalen	Nordfjord	monzonite	RA	0.4	5.22	0.08	6.04	0.13	^{14}C	4.0	Nesje (2002)
38	Bøyadalen	Fjærlandsfjord	monzonite	RA				3.5	0.6	^{10}Be	8.1	Hermanns *et al*. (2011)
39	Øyrahagestolen	Fjærlandsfjord	gneiss	RA				10.0	1.4	^{10}Be	1.6	Hermanns *et al*. (2011)
40	Uraneset	Fjærlandsfjord	gneiss	RA				10.1	1.4	^{10}Be	1.5	Hermanns *et al*. (2011)
41	Skjeringahaugane P1	Lusterfjord	phyllite	RS				7.0	0.8	^{10}Be	3.0	Hermanns *et al*. (2012)
42	Skjeringahaugane P2	Lusterfjord	phyllite	RS				6.8	0.7	^{10}Be	3.2	Hermanns *et al*. (2012)
43	Skjeringahaugane P3	Lusterfjord	phyllite	RS				4.0	0.6	^{10}Be	6.0	Hermanns *et al*. (2012)
44	Storurdi	Urdadalen	pyroxene-granulite	RA	10			1.83	0.76	SHD	7.5	Wilson (2009)
45	Aurlandsfjorden	Aurlandsfjorden	phyllite, granodiorite	RA		2.64	0.07	2.77	0.06	^{14}C	8.2	Bøe *et al.* (2004)
46	Stampa (Joasete)	Flåm	phyllite	RA	4.27			3.754	0.38	^{10}Be (4)	7.0	Böhme *et al*. (2013)
47	Stampa (Ramnanosi 1)	Flåm	phyllite	RA	0.3			2.579	0.22	^{10}Be (4)	8.2	Böhme *et al*. (2013)
48	Stampa (Ramnanosi 2)	Flåm	phyllite	RA	2.71			12.87	1.12	^{10}Be (4)	0	Böhme *et al*. (2013)
	Telemark											
49	Urdbøuri	Rauland	granite, granodiorite	RA				11.3	1.3	^{10}Be	1.0	Hermanns *et al*. (2017a)

Notes:

1. Type: RA rock avalanche; RF rockfall; RS rockslide; DSGSD deep-seated gravitational slope deformation.
2. Volume calculations are often approximations based on surficial area and average thickness of the deposits (or extracted from swath bathymetry and seismic surveys for fjord sediments).
3. Method:

(i) ^{10}Be cosmogenic exposure ages were calculated by cited authors using the CRONUS (Balco *et al.*, 2008) and are reported here as mean ages and ±1 sigma uncertainties. Unless otherwise stated, ages were calibrated to global production rates and Sa (LSDn) scaling models according to Lifton *et al.* (2014) and Borchers *et al.* (2016). Derivation of ^{10}Be ages from local production rates (Fenton *et al*., 2011; Goehring *et al.*, 2012) would make the ages approximately 10% or 5% older, respectively (Hermanns *et al.,* 2013b).
(ii) STR refers to age estimation based on morpho-stratigraphic relations.
(iii) For consistency, radiometric ^{14}C ages were re-calibrated to calendar (cal.) years B.P. using the IntCal13 dataset (Reimer *et al.*, 2013), at the ±1 sigma uncertainty level.
(iv) SHD (Schmidt hammer exposure dating) was undertaken using Type N hammers and local calibration curves.
4. These authors derived ^{10}Be ages using St scaling (Lal, 1991; Stone, 2000).
5. Lag time represents the maximum difference between the calibrated ages of local deglaciation and RSF at each locality.

archive (Longva et al. 2009), and Matthews et al.'s (2018) record of small RSFs in Jotunheimen.

Chronological control for 34 sites was established by terrestrial cosmogenic nuclide (^{10}Be) exposure dating, described in the source references. ^{10}Be cosmogenic exposure ages were calculated by the cited authors using the CRONUS (Balco et al. 2008) and are reported here as mean ages and ±1 sigma internal uncertainties. Unless otherwise indicated, ages were calibrated to global production rates and Sa (LSDn) scaling models according to Lifton et al. (2014) and Borchers et al. (2016). Eight further samples were dated through ^{14}C analyses of organic material sampled from terrestrial deposits or cores of fjord sediments. For consistency, all radiometric ^{14}C ages were re-calibrated to calendar (cal.) years B.P. using the IntCal13 dataset (Reimer et al. 2013), at the ±1 sigma uncertainty level. Where multiple dates had been secured at a given site, a 'best-estimate' age for the dated RSFs was obtained by calculating the uncertainty-weighted mean age for each RSF. The ages of four landforms were estimated by Schmidt hammer exposure dating (SHD), and three deposits were dated by morphostratigraphic correlation (Table 5.1).

Aggregation and more detailed interrogation of these datasets is ongoing, and forms part of a broader project. The distribution of ages (A) of the 49 dated RSFs are plotted with the cumulative number of RSFs (N) in Fig. 5.12, and are described by the regression equation:

$$N = 3.7583A - 5.2945 \quad (n=49, r^2 = 0.993) \qquad (1)$$

The data demonstrate that RSF activity has occurred throughout almost the entire postglacial period, from 15.4 ± 1.7 ka to 1.0 ± 0.4 ka. The frequency of activity, however, was non-linear through time, with the cumulated number of RSFs increasingly slightly more steeply with age at ~12.1 ka, 10.1 ka, 7.2 ka and 5.3 ka, than during intervening periods. The periodicity for RSFs during these episodes is extremely high, for example between ~12-11 ka, 10-9 ka and 5.3-4.9 ka, the sampled RSFs occur on average every ~130 years. This compares with an overall average periodicity of ~310 years for all 49 RSFs since ~15 ka. Fig. 5.13a plots the frequency of RSFs per millennia.

The timing of deglaciation, however, varies from ~9.9 ka (for inland, high-elevation sites that were reoccupied by glacier ice during the Younger Dryas) to ~14.2 ka (for coastal localities

in Mør og Romsdal, that were first to emerge from the retreating Scandinavian Ice Sheet). Fig. 5.13b takes account of these differences, depicting the distribution of RSF ages since ice retreat for each site, aided by recent, time-slice reconstructions of ice retreat (Hughes *et al*. 2016).

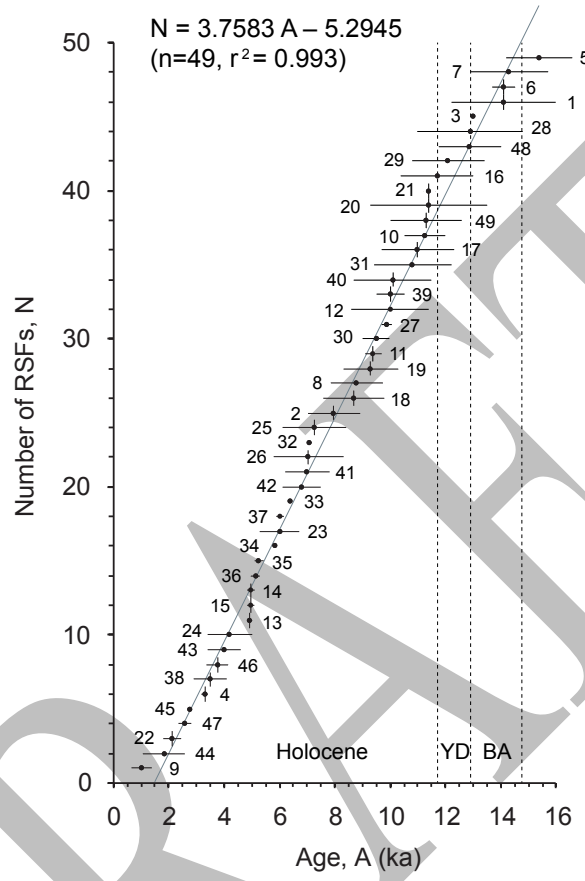

Fig. 5.12. Calibrated ages for 49 RSFs, arranged cumulatively by ascending RSF age. Numbering follows Table 5.1. Length of the horizontal bars represent ±1σ total uncertainties, and vertical bars indicate weighted mean ages. The number of RSFs (N) increases non-linearly with increasing age (A). Vertical dashed lines separate the Bølling-Allerød Interstadial (BA: 14.7–12.9 ka), Younger Dryas Stade (YD: 12.9-11.7 ka) and Holocene (<11.7 ka).

Fig. 5.13b reveals a fascinating temporal distribution of RSFs. The immediate response of recently deglaciated rock-slopes to nonglacial conditions appears comparatively muted. Only 12% of total postglacial failures took place in the first millennium after ice retreat, though subsequently there is an intensification of RSF activity, with nearly one-third of recorded failures having occurred 1-3 ka following deglaciation. RSF frequency then experienced an overall decrease over a duration of 4 ka. Some 7-6 ka after ice retreat, however, Holocene RSF activity accelerated rapidly, and 20% of postglacial failure occurred at these times (~4-5 ka and 7-8 ka BP). Since ~4 ka BP RSF frequency declined markedly. This pattern resonates

with McColl's (2012) global survey of major RSFs, in which some major failures were shown to have initiated prior to or synchronous with deglaciation, while most documented cases typically occurred some millennia after ice retreat.

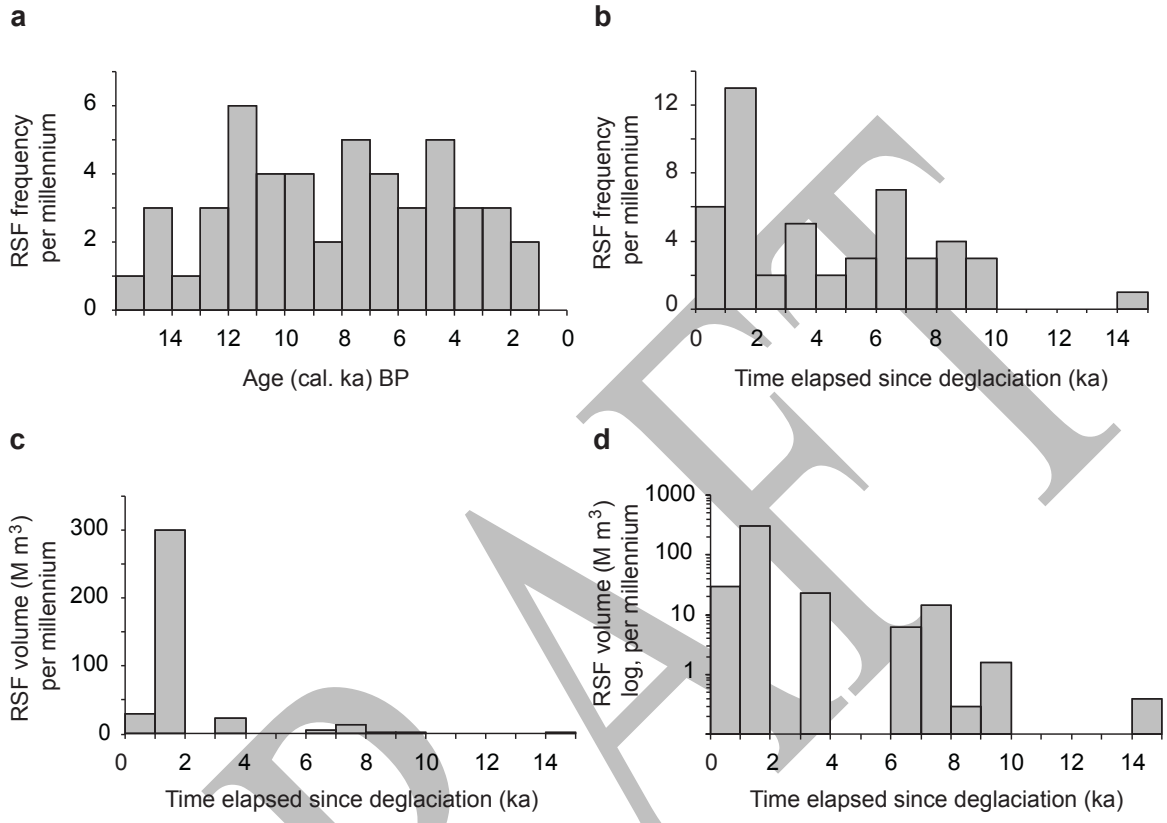

Fig. 5.13. Temporal distribution of the ages of 49 dated RSFs in western Norway: (a) frequency of the number of RSFs per millennium; (b) frequency of the number of RSFs per millennia since local deglaciation; (c) total RSF volume failed per millennium since local deglaciation; and (d) total log RSF volume failed per millennium since local deglaciation.

It is instructive to further evaluate the RSF timing data by considering the volume of material reworked, as well as event frequency, as estimated for many of the sampled RSF deposits. Figures 14c and d illustrate the findings, which resonate with those of Böhme et al. (2015). While both magnitude and frequency of RSFs during the initial stages of deglaciation appear to have been somewhat subdued, some 80% of total postglacial rock-slope sediment flux appears to have been released from unstable and metastable stores during the second millennia after ice retreat. Of course, volume calculations are rough estimations. Smaller events may be under-represented for older time periods, with their signature more likely to have been removed by erosion or hidden by larger deposits (Böhme et al. 2015). Notwithstanding some occasional exceptions, though, the prehistoric record after 10 ka is

dominated by RSF events whose individual and cumulative volume were several orders of magnitude lower than during the early paraglacial period.

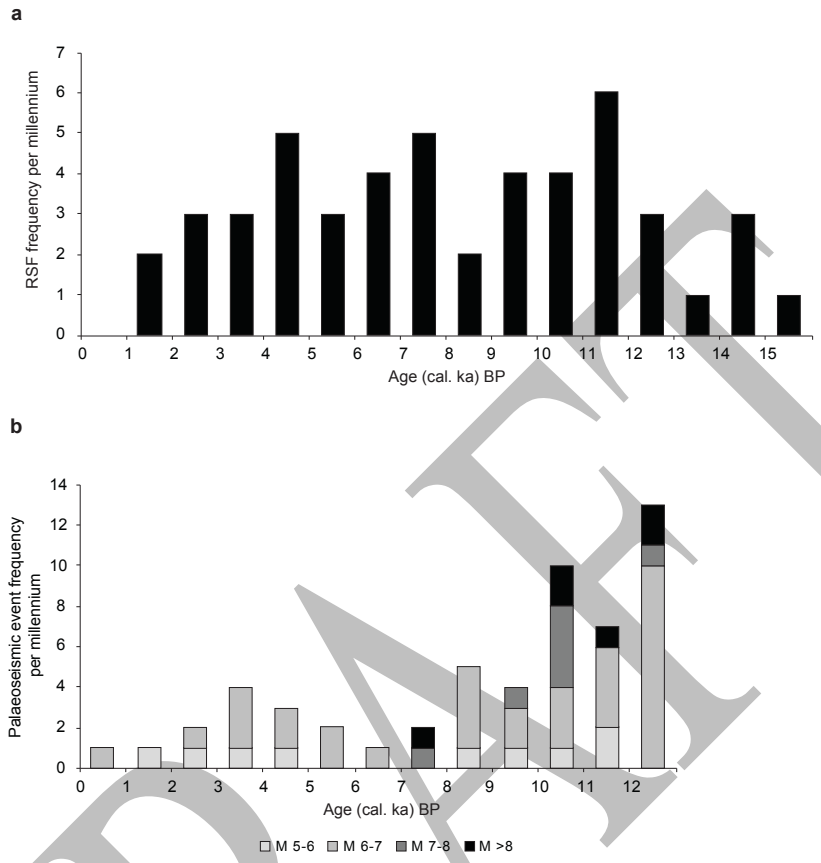

Fig. 5.14. Comparison of (a) west Norwegian RSF activity (this study) with (b) the paleoseismic record of Sweden (Mörner 2013).

Proposed long-term and short-term causes of RSF activity are considered below, in the light of these observations.

Glacial debuttressing and thermal shock

In contrast to a rapid (century-timescale) response to deglaciation, many major RSF events in western Norway evidently lagged deglaciation by ~1-2 ka (Blikra et al. 2006; Böhme et al. 2015). Furthermore, as suspected by workers in Norway for some time, the frequency (not magnitude) of RSF activity appears to have reached levels comparable with the Late Weichselian/Holocene transition as recently as 4 ka (Blikra et al. 2006). These characteristics of the Norwegian dataset contrast with models that envisage paraglacial rock-slope adjustment in terms of an immediate 'rapid response' to deglaciation, succeeded by

approximately constant event frequency averaged over the timescale of interglacial recovery. In particular, apart from six (12%) cases of dated RSFs that were synchronous with deglaciation, the patterns summarised in Table 5.1 do not fit well with 'deglacial debuttressing' or 'paraglacial thermal shock', given the close association of these mechanisms with rapid collapse of unstable rockwalls during or immediately after glacier downwastage.

Paraglacial stress release

Conversely, the majority of large failures observed in this inventory have post-dated ice retreat by at least one thousand years. Paraglacial stress release is the development of stresses perpendicular to and parallel to a rock slope that result from glacial erosion and deglacial unloading (McColl 2012). Such time-dependent stress changes may initiate gradual rock mass fatigue over century to millennial timescales through progressive shear plane development within fractured rock masses. As noted, for example, at Ivasnasen (Oppikofer et al. 2017), slope instabilities may 'endure' slow deformation over such timescales. Modelling the response of glacially-oversteepened slopes to Pleistocene deglaciation in Canada suggests that average pre-failure endurance may locally exceed 5 ka (Cruden and Hu 1993).

An implication of this interpretation is that the observed pattern of timing of RSFs in Fig. 5.13 may reflect prolonged stress release initiated by Late Weichselian unloading. Such time-dependant degradation of rock strength may result in spontaneous kinematic release of rock centuries or millennia after deglaciation, with or without involvement of an extrinsic trigger mechanism.

This explanation for the delayed, or lagged response of rock-slope systems is consistent with the behaviour of at least 19 (39%) of the sampled RSFs that failed during the first 2 ka after deglaciation. Further research is needed to assess 'pre-failure endurance' as an explanation for these substantial time-lags, and to identify its temporal limits across a range of geotechnical and lithological contexts. One may speculate further whether the clustering of dated RSFs 7-6 ka after deglaciation (i.e. at ~4-5 ka and 7-8 ka BP) may represent a renewed cycle of stress release failures, caused by intense 'paraglacial erosional unloading' of rockwall surfaces and consequent rock-mass degradation 7-5 ka earlier.

Alternatively, periodic renewal of recorded RSF events at ~7-8 and 4-5 ka suggests that other factors may trigger failure of these glacially-conditioned rock-slopes. While triggering mechanisms for large rock avalanches in the region remain poorly understood, Blikra et al. (2002) cite high-amplitude earthquakes and extreme rainfall events as the most likely important factors.

Seismic shocks

Depending on their pre-existing state, powerful (M >6) earthquakes can weaken rock masses and trigger catastrophic RSFs (Keefer 1984; Eisbacher and Clague 1984; Jibson 1996) and smaller shocks may trigger smaller failures.

Although the seismicity of Norway is low to intermediate in intensity, and magnitudes rarely exceed 5.5 (Fjeldskaar et al. 2000), it is likely that earthquake activity was much greater during Late Pleistocene deglaciation. A pulse of shallow crustal seismic activity can be attributed to differential postglacial crustal rebound and associated shallow faulting, in conjunction with elastically stored tectonic stresses (Cave and Ballantyne 2016). The prolonged response time of resultant crustal stress changes mean that associated seismic activity may lag deglaciation by centuries or millennia (Stewart et al. 2000).

Notwithstanding Norway's poorly controlled paleoseismic records (Redfield and Hermanns 2016), paleoseismological studies suggest that large-magnitude (>6 M) intraplate earthquakes occurred in Scandinavia at ~13–9 ka (Mörner 2005, 2013), which correlates with the peak rate of postglacial uplift in western Norway (Svendsen and Mangerud 1987; Fjeldskaar 1997). Of 53 M>6 palaeoearthquakes in Sweden (Mörner 2013, and references therein), 28 occurred between 11-9 ka (averaging 14 ka^{-1}), compared with 21 earthquakes for the last 9 ka (at an average rate of 2.3 ka^{-1}). Six out of seven M>7 earthquakes occurred during regional deglaciation, 13-9 ka.

This pattern was also observed in west and mid-Norwegian fjords, with frequent earthquakes inferred during the Early Holocene (~11.2-8.3 ka) and triggered by glaco-isostatic rebound, followed by low frequency in the Mid Holocene, and a slight reactivation in the Late Holocene with clusters from 4.2-1.8 ka (Bellwald et al. 2019). Late Holocene seismic reactivation has been observed in all regions previously covered by the Scandinavian Ice

Sheet. Analysis by Bellwald *et al*. (2019) of 125 postglacial mass movement deposits (subaquatic mass flows, debris flows, slumps, slides and turbidites) in western Norwegian fjords led to the identification of clusters of enhanced activity in the Early Holocene (11-9.7 ka), at around 8.0 ka, and in the Late Holocene (~4.2 ka to present). The authors interpreted most of these events as reflecting regional seismic activity triggering failure of climatically-preconditioned slopes. Interpreting their record of mass movement clusters as a proxy for palaeoseismic activity, they suggest that at least 36 individual regional earthquakes (M >6) occurred in west and mid-Norway through the Holocene.

Coastal areas of western Norway represent the region of greatest historic earthquake activity in the south of the country (Dehls et al. 2000b). Moreover, the concentration of gravitational faults and slope failures in Sogn og Fjordane and Hordaland, and in parts of Møre og Romsdal may point to powerful prehistoric earthquakes in western Norway (Olesen et al. 2004, 2013; Olsen et al. 2013). However, triggering mechanisms for a cluster of large RSFs in Innfjord (Møre og Romsdal), formerly attributed to Holocene neotectonic seismicity and earthquake shaking (Anda *et al*. 2002; Blikra et al. 2006) require fresh evaluation following re-interpretation of a supposed Holocene reverse fault (the so-called Berill Fault) by Schleier et al. (2016).

If palaeoseismicity played a significant role in triggering postglacial RSFs in western Norway, a close correspondence between the observed RSF ages (Table 5.1) and the timing of rapid, regional postglacial uplift and palaeoearthquakes might be expected. Many RSFs within a given radius would occur on or shortly after the same day. At ±1σ uncertainties, the calibrated age ranges for 28 (57%) of events in the RSF dataset are bracketed by or overlap one of the aforementioned periods of enhanced postglacial seismicity in western Norway (11.2-8.3 ka and 4.2-1.8 ka). However, many of these ages also overlap with other likely triggers and causal factors, notably the period of assumed paraglacial stress-release. Initial comparison of the RSF database and the regional plaeoseismic record suggests only weak association (Fig. 5.14).

Climatic triggers

As indicated above, changes in rockwall hydrology and thermal regime may have a critical bearing on rock-slope instability (Fig. 5.15), via postglacial permafrost melt, as well as

seasonal snowmelt, extreme rainstorms and weathering of shear surfaces (Krautblatter et al. 2013; Blikra and Christiansen 2014; Schleier et al. 2015; Hilger et al. 2018). At present, permafrost in western Norway may exist to considerable depths in rockwalls above 1,300-1,700 m elevation, depending on aspect (Hipp et al. 2014). During the Younger Dryas, permafrost probably extended to sea-level, so rock-mass stability during and shortly after deglaciation would likely have been compromised via excess joint-water pressures induced by permafrost degradation. Schleier et al. (2015) explored this idea further, with regard to the dating evidence from Innerdalen (Møre og Romsdal). The rock avalanche events they documented occurred during the Late Pleistocene Bølling-Allerød Interstadial (~14.7–12.9 ka) under paraglacial conditions, and during the Atlantic chronozone, or Holocene Thermal Maximum (~8–5 ka). The authors observed that both events immediately followed significant cooling periods in the northern hemisphere (Older Dryas stadial 14.1-13.8 ka and the so-called 8.2 ka event), when the permafrost limit was lowered, and likely contributed to greater rockwall stability. However, during the subsequent warming periods, rising permafrost limits are considered to increase the probability of failure. As outlined above, Matthews et al. (2018) also highlighted Holocene permafrost degradation as a conditioning factor for small RSFs; a finding that carries important implications for slope instability under future warming scenarios.

Permafrost degradation was tested as an explanation for periodic increases in rock-slope activity by interrogating the timing data in Table 5.1. Very rapid warming occurred twice during the postglacial period, terminating stadial conditions at the Older Dryas Stade - Bølling-Allerød Interstade transition (~14.7-14.2 ka) and at the Younger Dryas Stade - Holocene transition (~12.2-11.7 ka). Rapid warming also characterised the transition towards the Holocene Thermal Maximum (~8.5-8.0 ka). Each of these periods likely caused permafrost degradation, increased joint-water pressure and enhanced freeze-thaw activity (Ballantyne *et al*. 2013; McColl 2012). However, the number of RSF age ranges (±1σ) that overlap these three periods of rapid warning (19) is actually lower than those that occur within the subsequent 500 years after these warming transitions (23). Accordingly, the present database gives no clear evidence for widespread RSF activity having been triggered by warming and thaw of permafrost and/or increased water pressure within rock masses. The timing of the majority of dated RSFs appears to be independent of periods of rapid warming.

Fig. 5.15. The 20 m high backscarp crowning the Mannen rock-slope instability, Møre og Romsdal. The site is classified high-risk by the Geological Survey of Norway (NGU), owing to deformation rates of 2-5 cm per year of ~5 x 10^6 m^3 rock mass. Seasonal acceleration at the sliding surface occurs at the end of the summer, when local ground temperatures exceed 0°C. Extensive, prehistoric rock avalanche deposits litter the Rauma (Romsdalen) valley floor some 1,200 m below and represent 6-9 catastrophic RSF events dated to ~12-4.5 ka (Hilger *et al.* 2018). With the summit (1,294 m) corresponding with the lower limit of permafrost, near-future warming is expected to further lower rock-mass stability at this and similar sites. Photo: Paula Hilger.

However, mechanical modelling of permafrost degradation by Krautblatter et al. (2013) suggests that permafrost degradation may slowly condition RSF activity on long-term (millennial) timescales, by both external controls (via gradual and cyclical thermal changes during the glacial-interglacial transition), and internal responses (via progressive rock fatigue and joint propagation). In consequence, thermal effects should not be dismissed as triggering or preparing a higher number of RSF events than those bracketed by these narrow windows of rapid warming.

Nesje et al. (1994) and Nesje (2002) speculated whether climatic deterioration (cooler and wetter climate with enhanced seasonality) following the post-Holocene Thermal Maximum may have initiated three Mid-Holocene rock avalanches dated to ~4.2 and 6.0 ka in Oldedalen (Sogn og Fjordane) and at ~6.0 ka in Norangsdalen (Møre og Romsdal), via

elevated joint-water pressures. Precipitation in southern Norway was 170% greater at ~6-5 ka than during the reference period 1961–1990 (Bøe et al. 2006).

The significance of high, fluctuating groundwater within bedrock is powerfully exemplified in the case of the 1756 Tjellefonna (Møre og Romsdal) rockslide, which followed two weeks of heavy rain (Furseth 2006). Numerical slope stability modelling and historical accounts suggest that heavy, long-lasting rainfall was the triggering factor for this slide, the largest (9.3–15 M m^3) RSF historically recorded in Norway (Sandøy *et al* 2017). Climatic deterioration (higher precipitation connected to a strong seasonality) at the end of the Holocene Thermal Maximum (when permafrost distribution was at a minimum) has also been proposed as a possible explanation for temporal clustering of multiple failures at Mannen (Møre og Romsdal) at ~5.5-4.5 ka (Hilger et al. 2018).

However, the millennial-scale delay between deglaciation and peak failure frequency at the sampled RSFs implies that high joint-water pressures associated with deglaciation played a limited part in triggering failure at these sites. Nonetheless, increased precipitation during periodic climatic deterioration may account for some of the RSF ages during the Mid-Late Holocene, such as the frequency peaks at ~5-4 ka. As described above, regional climatic irregularities causing increased rainfall have been tentatively linked to enhanced colluvial reworking of sediments in western Norway at 5.6-5.3 ka and 3.2-2.8 ka. However, none of the calibrated ages of observed RSFs in Table 5.1 fall within these periods, and only five (10%) of the ±1σ age ranges exhibit any overlap with these periods of apparent enhanced rainfall.

Nonetheless, a lack of temporal connection between RSF events and phases of enhanced precipitation does not necessarily exclude specific, short-term meteorological events that may have prepared or even triggered failure (*cf.* Ostermann and Sanders 2017). Further analysis of the timing data and regional climatic records may facilitate more robust evaluation of this and other climatic triggers.

Temporal patterns: summary

In general, the results of this preliminary analysis support those from previous research in the European Alps (Prager *et al*. 2008, McColl 2012) and Scotland (Ballantyne et al. 2014a, b)

indicating that the wastage of Late Pleistocene ice sheets in tectonically-stable montane regions was followed by a period of greatly enhanced RSF activity that extended over several millennia. The most important factors for preconditioning and triggering failure appear to have been paraglacial stress release, progressive rock-mass weakening, and possibly seismic activity driven by rapid rates of glacio-isostatic rebound during the period of maximum uplift rates. Glacial debuttressing and climatic factors appear to have been of more limited, local importance in triggering postglacial RSFs in northern and central Europe, though the relationship between rockwall thermal changes, increased water supply and Late Holocene RSF activity in Norway merit further attention.

5.6 Modelling RSF frequency through time

Four general models have been proposed (Ballantyne and Stone 2013) for changing RSF frequency with time elapsed since deglaciation (Fig. 5.16), namely (1) constant frequency (steady state) model (the frequency of RSFs does not change with time; Cruden and Hu 1993); (2) steady state decline model (the frequency of RSF activity declines linearly over time; (3) exhaustion model (the frequency of RSF activity declines exponentially as sediment sources ('unfailed' metastable rockwalls) are depleted; Cruden and Hu 1993); and (4) rapid response model (the frequency of RSF activity is greatest during or immediately after deglaciation; Church and Ryder 1972).

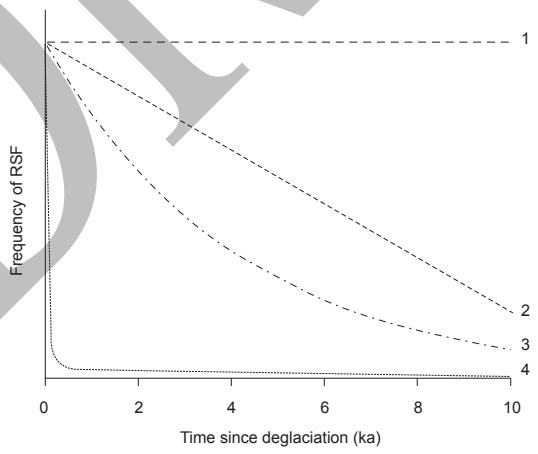

Fig. 5.16. Four possible models for the changing frequency of RSF activity after deglaciation: 1. constant frequency model; 2. steady-state decline; 3. exhaustion model; 4. rapid response model. For explanation, see text. Source: Ballantyne and Stone 2013, Fig. 1.

The value of these general models of paraglacial landscape response lies in their simplification and generalisation of complex realities. By definition, therefore, they hide much of the local variability related to specific environments and process domains (Cossart et al. 2013), which becomes increasingly relevant as the scale of inquiry is reduced (Kirkbride and Deline 2018). In identifying a number of unresolved paraglacial research priorities, Olivia *et* al. (2019) highlight modelling of complex paraglacial landscape response and sediment cascades to allow landscape trajectories to be anticipated and their effects managed.

Collection of a large inventory of published RSF ages spanning the Late Weichselian-Holocene has facilitated evaluation of these models (Fig. 5.17). The timing data presented fail to conform closely to any of the proposed models, but suggest that the temporal distribution of postglacial RSFs is best described by a modification of the exhaustion model that incorporates episodic, external perturbations and renewed, stochastic, paraglacial responses. Fig. 5.17b illustrates a proposed 'episodic response model'. While Ballantyne (2002a) outlined a visually similar scheme for the episodic release of glacially-conditioned sediment, exemplified in the case of a marine transgression through primary glacigenic deposits, there are important distinctives.

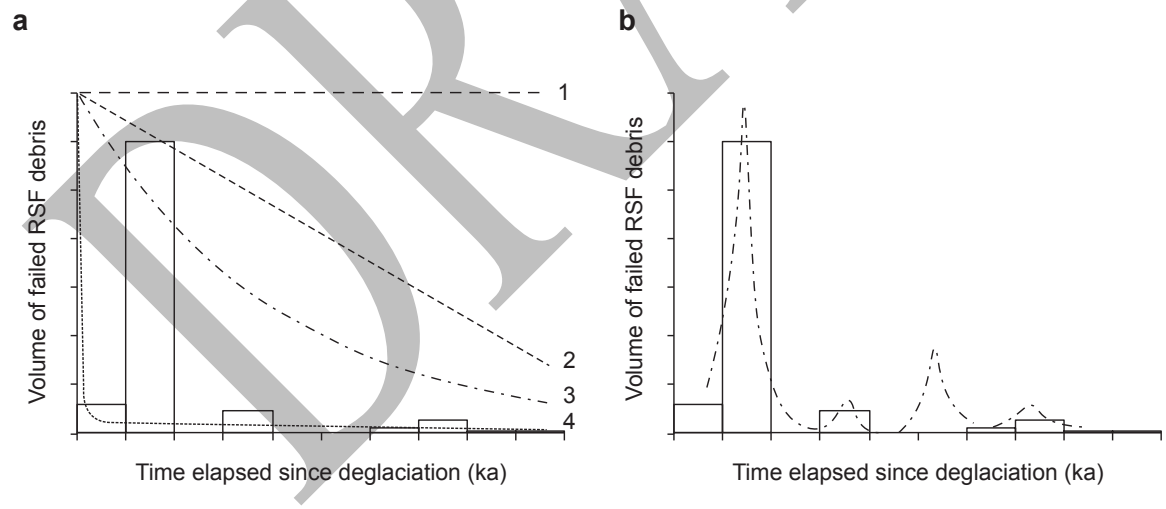

Fig. 5.17. Different models of time-dependent behaviour of postglacial RSF activity have been fitted to the volume distribution of failed RSF debris, described in this study, but fail to account sufficiently for the observed post-deglaciation time lag. (b) In contrast, a model following an episodic response to deglaciation shows the best fit for the dataset, and presents multiple possible pathways for subsequent delayed or renewed RSF activity, as is widely observed in deglaciated mountain environments.

In recent decades since exhaustion curves were first applied to paraglacial rock-slope systems, the temporal complexity of the latter has become increasingly evident. In particular, greater attention has been given to pre-failure endurance and the post-deglaciation time lag that appear to characterise many (but not all) rock-slope systems (McColl 2012; Ballantyne et al. 2014a, b). Modelling rock-slope responses to deglaciation must accommodate these different trajectories.

The episodic response model presented here also rejects an assumption of the exhaustion model that each site fails only once. As outlined above, multiple, closely-spaced, large RSFs have occurred on the same slope at several localities in Norway. The work outlined in this chapter also tentatively proposes that the history (memory) of failure at a given site may increase the likelihood of repeat failures by exposing fresh, unloaded, metastable bedrock surfaces and joint networks and reorganising stress fields (*cf.* Crosta et al. 2017; Hilger et al. 2018).

Further, the probability of failure at any given site is not constant, and supply of metastable and available material changes spatially and over time, and is to a limited extent, replenishable. Valley impoundment by RSF debris may lead to localised fluvial aggradation (upstream) and enhanced incision adjacent to and downstream of RSFs, thereby increasing slope instability and metastable sediment availability with time (Rodríguez-Rodríguez *et al*. 2018; Olivia et al. 2019).

The index for illustrating the magnitude and direction of paraglacial response is therefore measured in terms of volume of failed RSF debris rather than sediment availability, which can vary spatially and temporally over an interglacial timescale. While sediment cascades represent unifying conceptual frameworks for postglacial landscape evolution, often in terms of an exponential decay in paraglacial sediment supply through time, the episodic response model gives attention to these non-uniform and complex elements of paraglacial rock-slope adjustment.

5.7 Future Research

Although the Norwegian montane landscape is dominated by the distinctive signature of recurrent Pleistocene glaciation, a range of postglacial geomorphological responses has led to

extensive modification of the glacial landscape. Explicit recognition of the nature and effects of this glacially-conditioned landscape evolution is relatively new, and significant gaps in our understanding remain. This section presents a number of exciting avenues for future study of rock-slope activity in glaciated mountain regions, particularly in Norway.

The research outlined in this chapter provides clear empirical evidence for glacially-influenced or conditioned RSF activity in western Norway. The spatio-temporal distribution of prehistoric failures imply that multiple, temporary increases in RSF activity occurred at different times following deglaciation, characterised by varying amplitude, duration and geomorphic work. While the initiation of paraglacial rock-slope adjustment to deglaciation can be very rapid (Kos et al. 2016), a widely observed (but only partly understood) characteristic of many deglaciated rock-slope systems is the significant time lag between glacier retreat and maximum RSF activity. To better explain these lags McColl (2012) recommends attention is focused on (i) assessing the timescale of stress redistribution and development of rock mass degradation, (ii) evaluating the links between RSF event distribution and climate data (periodic warming and increased rainfall) and (iii) with enhanced postglacial seismicity. Cosmogenic dating of fault scarps will shed further light on the temporal connection between palaeoseismicity and enhanced RSF activity.

The heterogeneous spatial distribution, magnitude and mechanics of RSF events within mountain landscapes reflect a complex interplay of multiple causal factors that collectively define the sensitivity of rock-slopes to fail at different scales, and yet vary in their relative importance between different scales. Multivariate modelling approaches (e.g. multiple logistic regressions) are being successfully applied to explaining the complex system behaviour of multiple, scale-dependent controls on rockfall (e.g. Messenzehl et al. 2017), and may represent a fruitful approach to improving our understanding of the relative significance of RSF controls, and effective hazard management.

Integrating advances in geochronology, geodetics and remote survey and visualisation tools have facilitated the development of regional-scale RSF inventories that allow research to extend beyond reductionist, landform-based enquiries to better explain (and predict) the mechanics and evolution of mountain landsystems. Monitoring of unstable rockwalls has yielded clearer insights into the drivers of slope failure and deformation, and allows calibration of slope stability models for back-analyses of former failure. Combining

analytical or numerical modelling with field monitoring of contemporary mechanisms therefore represents an important approach for improved simulation and understanding of complex, multiple causes of failure, as well as assessment of 'pre-failure endurance' as an explanation for millennial-scale time-lags.

Several studies illustrate the rich potential of coupling onshore and offshore datasets to gain more representative overview of temporal and process variability, vital for accurate assessment of former and future hazards. Analysis of fjord deposit inventories (e.g. Longva et al. 2009; Böhme et al. 2015) demonstrate well the potential of lake and offshore archives for deciphering histories of multistage RSFs that may be camouflaged in subaerial settings (Knapp et al. 2018) or erased by subsequent (e.g. Younger Dryas) ice advances.

To date, systematic analysis of the spatial controls on Norwegian rock slope instabilities is limited to three counties (Møre og Romsdal, Sogn og Fjordane and Troms). Understanding these parameters and prediction of potential RSF events will be reinforced by extending this approach more widely.

The spatio-temporal distribution of rockfall talus-derived landforms (protalus rock glaciers and pronival (protalus) ramparts) also promises to shed light on the occurrence, magnitude and frequency of small RSFs in western Norway (e.g. Lilleøren and Etzelmüller 2011). Establishing the age and extent of these features may clarify understanding of rockfall and small-scale RSF activity in western and southern Norway, though their history may represent protracted, multi-stage activity conditioned by multiple factors of varying importance.

Finally, the research summarised in this chapter provides compelling evidence of the efficiency of paraglacial rock-slope activity for dismantling mountain slopes after deglaciation. Vast quantities of coarse debris are frequently released within the first few millennia of ice retreat, and accumulate in valley-floor or fjord stores prior to further glaciation. The implications for interpreting postglacial sediment budgets, and evaluating the role of paraglacial RSF activity for glacial trough widening, cirque enlargement, and subsequent glacial erosion, merit further consideration.

5.8 Summary

The findings of this synthesis are broadly congruent with wider research that emphasises the persistence and transient nature of the paraglacial period in rock-slope systems. The following conclusions are highlighted:

1. Deglaciation marks a complex transition of boundary conditions for rock slope stability in which steep, unstable bedrock stores respond non-linearly to glacial inheritance. Most prehistoric RSFs in the heavily glaciated terrain of western Norway can be considered 'paraglacial' in the sense that they have occurred in a transitional period of environmental adjustments following the disturbance of deglaciation and involve changes in the intensity of landscape-forming processes (Oliva et al. 2019). Although they were not directly caused by glaciation, they would not have occurred without prior glacial erosion.
2. Failure generally involves a complex, multi-phase interplay of internal (rock mechanical and topographic parameters, subcritical fracture propagation) and external (climate-controlled joint-water pressures and thermal cycles, and seismic) factors at different spatial and temporal scales.
3. The high concentration of tectonic deformation structures in western Norway, and the high relief that characterises regional terrain, are important parameters that precondition rock slope susceptible to the development of large rock-mass deformations and failures.
4. Preliminary analysis of the frequency and volume of 49 published RSF ages in western Norway suggests a modest increase in major RSF activity occurred during or immediately after Late Weichselian deglaciation.
5. Time-dependent paraglacial stress release and progressive rock mass degradation, in combination with glacio-isostatic crustal adjustments and possibly large-magnitude earthquakes, appear to have played an essential role in preconditioning, preparing and triggering a much larger number of RSFs and gravitational deformation structures up to several thousand years after ice sheet decay. 80% of total RSF volume surveyed in western Norway appears to have been delivered to fjords and valley floors during a period ~1-2 ka after deglaciation.
6. Catastrophic RSF activity in western Norway has continued through the Holocene, suggesting that rock-slope response to deglaciation is not solely attributable to glacial debuttressing, postglacial seismicity and associated rock-mass weakening. High event frequencies were identified at 8-7 ka and 5-4 ka BP, though the volume of rock material

released during the Mid and Late Holocene was at least one order of magnitude lower than during the second millennium after deglaciation. These period of enhanced, delayed or time-lagged RSF activity are ascribed to Holocene climatic irregularities, including seismic activity, and possibly increased precipitation rates, high air temperatures and associated degradation of permafrost in rock-slopes.

7. Glacial and paraglacial inheritance, alpine relief, abundant brittle and ductile bedrock structures, seasonal heavy precipitation, snow melt and freeze-thaw cycles continue to render the fjords and valleys of western Norway vulnerable to RSF events. These hazards may increase under global change scenarios, especially in relation to permafrost degradation.
8. The timing data presented fail to conform to existing general models of changing paraglacial RSF frequency (rapid-response, constant frequency (steady state), exhaustion and stead-state decline), but are best described by a modification of the exhaustion model that incorporates episodic, external perturbations and renewed, stochastic, paraglacial responses. This 'episodic response model' recognises this complexity, as well as the post-deglaciation time lag and pre-failure endurance that appear to characterise many rock-slope systems.
9. Several future research priorities are identified, including (a) understanding the significant time lag between glacier retreat and maximum RSF activity, especially the need to assess the timescale of stress redistribution and development of rock mass degradation; (b) the application of multivariate modelling approaches to explaining complex behaviour of RSF controls; (c) the use of numerical modelling and field monitoring of failure mechanisms to simulate multiple causes of failure; (d) harnessing the potential of fjord deposit inventories for reconstructing RSF histories; (e) extending systematic surveying of spatial controls on rock-slope instabilities to other counties of Norway; and (f) evaluating the use of talus-foot landforms as potential inventories of rockfall and small RSF events. Finally, several wider implications of the research presented in this chapter are recognised for the evolution of glaciated, montane landscapes.

Acknowledgments

The author is especially grateful to Paula Hilger, John Matthews and Peter Wilson for kindly supplying photographs, and to Reginald Hermanns for giving valuable feedback on an early

draft. The author, however, is solely responsible for the final outcome. Technical support from Mr Aiden Bygrave is gratefully acknowledged.

References

Aa AR Sjåstad J Sønstegaard E Blikra LH (2007) Chronology of Holocene rock-avalanche deposits based on Schmidt-hammer relative dating and dust stratigraphy in nearby bog deposits, Vora, inner Nordfjord, Norway. The Holocene 17: 955–964

Aarseth I, Austbø P, Risnes H (1997) Seismic stratigraphy of Younger Dryas ice-marginal deposits in western Norwegian fjords. Norwegian Journal of Geology 77: 65-86

Abele G (1997) Influence of glacier and climatic variation on rockslide activity in the Alps. Paläoklimaforschung 19: 1–6

Agliardi F, Crosta GB, Zanchi A (2001) Structural constrains on deep-seated slope deformations kinematics. Engineering Geology 59: 83–102

Anda E, Blikra LH, Braathen A (2002) The Berill Fault - first evidence of neotectonic faulting in southern Norway. Norwegian Journal of Geology 82: 175-182

André M-F (2009) From climatic to global change geomorphology: contemporary shifts in periglacial geomorphology. In: Knight J, Harrison S (eds) Periglacial and Paraglacial Processes and Environments. Geological Society, London, Special Publications 320, pp. 5-28

Andreassen LM, Winsvold SH (eds) (2012) Inventory of Norwegian Glaciers. Norwegian Water Resources and Energy Directorate (NVE), Oslo, Rapport 38–2012

Augustinus PC (1995a) Rock mass strength and the stability of some glacial valley slopes. Zeitschrift für Geomorphologie 39: 55–68

Augustinus PC (1995b) Glacial valley cross-profile development: the influence of in situ rock stress and rock mass strength, with examples from the Southern Alps, New Zealand. Geomorphology 14: 87–97

Balco G, Stone JO, Lifton NA, Dunai TJ (2008) A complete and easily accessible means of calculating surface exposure ages or erosion rates from ^{10}Be and ^{26}Al measurements. Quaternary Geochronology 3: 174–195

Ballantyne CK (2002a) A general model of paraglacial landscape response. The Holocene 12 371-376

Ballantyne CK (2002b) Paraglacial geomorphology. Quaternary Science Reviews 21: 1935–2017

Ballantyne CK (2003) Paraglacial Landsystems. In: Evans DJA (ed) Glacial Landsystems. Edwin Arnold, London, pp. 432-461

Ballantyne CK (2008) After the Ice: Holocene Geomorphic Activity in the Scottish Highlands. Scottish Geographical Journal 124: 8-52

Ballantyne CK, Stone JO (2013) Timing and periodicity of paraglacial rock-slope failures in the Scottish Highlands. Geomorphology 186: 150–161

Ballantyne CK, Sandeman GF, Stone JO, Wilson P (2014a) Rock-slope failure following Late Pleistocene deglaciation on tectonically stable mountainous terrain. Quaternary Science Reviews 86: 144–157

Ballantyne CK, Wilson P, Gheorghiu D, Rodés À (2014b) Enhanced rock-slope failure following ice-sheet deglaciation: Timing and causes. Earth Surface Processes and Landforms 39: 900–913

Bellwald B, Hjelstuen BO, Sejrup HP, Haflidason H (2016) Postglacial mass movements and depositional environments in a high-latitude fjord system – Hardangerfjorden, Western Norway. Marine Geology 379: 157–175

Bellwald B, Hjelstuen BO, Sejrup HP, Stokowy T, Kuvås J (2019) Holocene mass movements in west and mid-Norwegian fjords and lakes. Marine Geology 407: 192-212

Benestad RE (2005) Climate change scenarios for Northern Europe from multi-model IPCC AR4 climate simulations. Geophysical Research Letters 32: L17704, 1-3

Blair RW (1994) Mountain and valley wall collapse due to rapid deglaciation in Mount Cook National Park, New Zealand. Mountain Research and Development 14: 347-358

Blikra LH, Nemec W (1993) Postglacial avalanche activity in western Norway: depositional facies sequences, chronostratigraphy and palaeoclimatic implications. Paläoklimaforschung 11: 143-162

Blikra LH, Braathen A, Anda E, Stalsberg K, Longva O (2002) Rock avalanches, gravitational bedrock fractures and neotectonic faults onshore northern west Norway: Examples, regional distribution and triggering mechanisms. NGU Rapport 2002.016. Geological Survey of Norway, Trondheim, Norway

Blikra LH, Longva O, Braathen A, Anda E, Dehls JF, Stalsberg K (2006) Rock slope failures in Norwegian fjord areas: examples, spatial distribution and temporal pattern. In: Evans SG, Scarawcia Mugnozza G, Strom AL, Hermanns RL (eds) Landslides from Massive Rock Slope Failure: Proceedings of the NATO Advanced Research Workshop on Massive Rock Slope Failure: New Models for Hazard Assessment, Celano, Italy, 16-21 June 2002

(NATO Science Series: IV Earth and Environmental Sciences; 49) Springer, Dordrecht, pp. 475–496

Blikra LH, Christiansen HH (2014) A field-based model of permafrost-controlled rockslide deformation in northern Norway. Geomorphology 208: 34–49

Blikra LH, Majala G, Anda E, Berg H, Eikenæs O, Helgås G, Oppikofer T, Hermanns R, Böhme M (2016) Fare- og risikoklassifisering av ustabile fjellparti – Faresoner, arealhåndtering og tiltak. Rapport no. 77–2016. Norwegian Water Resources and Energy Directorate (NVE), Oslo (in Norwegian)

Bøe A-G, Dahl SO, Lie Ø, Nesje A (2006) Holocene river floods in the upper Glomma catchment, southern Norway: A high-resolution multiproxy record from lacustrine sediments. The Holocene 16: 445–455

Bøe R, Lepland A, Blikra LH, Longva O, Sønstegaard E (2002) Postglacial mass movements in western Norway with special emphasis on the 2000-2200 BP and 2800-3200 BP periods - final report. NGU Rapport 2002.020. Geological Survey of Norway, Trondheim, Norway

Bøe R, Rise L, Blikra LH, Longva O, Eide A (2003) Holocene mass movements in Trondheimsfjorden, Central Norway. Norwegian Journal of Geology 83: 3-22

Bøe R, Longva O, Lepland A, Blikra LH, Sønstegaard E, Haflidason H, Bryn P, Lien R (2004) Postglacial mass movements and their causes in fjords and lakes in western Norway. Norwegian Journal of Geology 84: 35-55

Böhme M, Saintot A, Henderson IHC, Henriksen H, Hermanns RL (2011) Rock slope instabilities in Sogn and Fjordane County, Norway: a detailed structural and geomorphological analysis. In: Jaboyedoff M (ed) Slope Tectonics. Geological Society, London, Special Publications 351, pp. 97-111

Böhme M, Hermanns RL, Fischer L, Oppikofer T, Bunkholt HSS, Derron M-H, Carrea D, Jaboyedoff M, Eiken T (2012) Detailed assessment of the deep-seated gravitational deformation at Stampa above Flåm, Norway. In: Eberhardt E, Froese C, Turner K, Leroueil S (eds) Landslides and Engineered Slopes. Protecting Society through Improved Understanding: Proceedings of the 11th International and 2nd North American Symposium on Landslides, Banff, Canada, 3-8 June 2012. Balkema, Rotterdam, pp. 647-652

Böhme M, Hermanns RL, Oppikofer T, Fischer L, Bunkholt HSS, Eiken T, Pedrazzini A, Derron M-H, Jaboyedoff M, Blikra LH, Nilsen B (2013) Analyzing complex rock slope deformation at Stampa, western Norway, by integrating geomorphology, kinematics and numerical modelling. Engineering Geology 154: 116-130

Böhme M, Derron M-H, Jaboyedoff M (2014) Quantitative spatial analysis of rockfalls from road inventories: a combined statistical and physical susceptibility model. Natural Hazards and Earth System Sciences Discussions 2: 81-121

Böhme M, Oppikofer T, Longva O, Jaboyedoff M, Hermanns RL, Derron MH (2015) Analyses of past and present rock slope instabilities in a fjord valley: implications for hazard estimations. Geomorphology 248: 464–474

Booth AM, Dehls J, Eiken T, Fischer L, Hermanns RL, Oppikofer T (2015) Integrating diverse geologic and geodetic observations to determine failure mechanisms and deformation rates across a large bedrock landslide complex: the Osmundneset landslide, Sogn og Fjordane, Norway. Landslides 12: 745-756

Borchers B, Marrero S, Balco G, Caffee M, Goehring B, Lifton N, Nishiizumi K, Phillips F, Schaefer J, Stone J (2016) Geological calibration of spallation production rates in the CRONUS-Earth project. Quaternary Geochronology 31: 188–198

Boulton GS, Dent DL (1974) The nature and rate of postdepositional changes in recently deposited till from south-east Iceland. Geografiska Annaler 56A: 121–134

Bovis MJ (1982) Uphill-facing (antislope) scarps in the Coast Mountains, southwest British Columbia. Geological Society of America, Bulletin 93: 804–812

Bovis MJ (1990) Rock-slope deformation at Affliction Creek, southern Coast Mountains, British Columbia. Canadian Journal of Earth Sciences 27: 243–254

Braathen A, Blikra LH, Berg SS, Karlsen F (2004) Rock-slope failures in Norway: type, geometry, deformation mechanisms and stability. Norwegian Journal of Geology 84: 67–88

Brierley GJ (2010) Landscape memory: the imprint of the past on contemporary landscape forms and processes. Area 42: 76-85

Bungum H, Lindholm C, Faleide J-I (2005) Postglacial seismicity offshore mid-Norway with emphasis on spatio-temporal-magnitudal variations. Marine and Petroleum Geology 22: 137–148

Cave JAS, Ballantyne CK (2016) Catastrophic Rock-Slope Failures in NW Scotland: Quantitative Analysis and Implications. Scottish Geographical Journal 132: 185-209

Church M (2002) Fluvial sediment transfer in cold regions. In: Hewitt K, Byrne M-L, English M, Young G (eds) Landscapes of Transition: Landform Assemblages and Transformations in Cold Regions. Springer Dordrecht, pp. 93–118

Church M, Ryder JM (1972) Paraglacial sedimentation: a consideration of fluvial processes conditioned by glaciation. Geological Society of America, Bulletin 83: 3059–3071

Church M, Slaymaker O (1989) Disequilibrium of Holocene sediment yield in glaciated British Columbia. Nature 337: 452–454

Cossart E, Fort M (2008) Sediment release and storage in early deglaciated areas: towards an application of the exhaustion model from the case of Massif des Écrins (French Alps) since the Little Ice Age. Norsk Geografisk Tidsskrift - Norwegian Journal of Geography 62: 115–131

Cossart E, Braucher R, Fort M, Bourles D, Carcaillet J (2008) The consequences of glacial debuttressing in deglaciated areas: Evidence from field data and cosmogenic datings. Geomorphology 95: 3–26

Cossart E, Mercier D, Decaulne A, Feuillet T (2013) An overview of the consequences of paraglacial landsliding on deglaciated mountain slopes: typology, timing and contribution to cascading fluxes. Quaternaire 24: 13–24

Cossart E, Mercier D, Decaulne A, Feuillet T, Jónsson HP, Sæmundsson Þ (2014) Impacts of post-glacial rebound on landslide spatial distribution at a regional scale in Northern Iceland (Skagafjörður). Earth Surface Processes and Landforms 39: 336–350

Crosta GB, Frattini P, Agliardi F (2013) Deep seated gravitational slope deformations in the European Alps. Tectonophysics 605: 13–33

Crosta GB, Hermanns RL, Dehls J, Lari S, Sepulveda S (2017) Rock avalanches clusters along the northern Chile coastal scarp. Geomorphology 289: 27–43

Cruden DM, Hu XQ (1993) Exhaustion and steady state models for predicting landslide hazards in the Canadian rocky mountain. Geomorphology 8: 279–285

Curry AM, Morris CJ (2004) Lateglacial and Holocene talus slope development and rockwall retreat on Mynydd Du, UK. Geomorphology 58: 85-106

Dadson SJ, Church M (2005) Postglacial topographic evolution of glaciated valleys: a stochastic landscape evolution model. Earth Surface Processes and Landforms 30: 1387–1403

Dahl S-O, Nesje A, Lie Ø, Fjordheim K, Matthews JA (2002) Timing, equilibrium-line altitudes and climatic implications of two early-Holocene glacial re-advances during the Erdalen Event at Jostedalsbreen, western Norway. The Holocene 12: 17–25

Dehls JF, Olesen O, Olsen L, Blikra LH (2000a) Neotectonic faulting in northern Norway; the Stuoragurra and Nordmannvikdalen postglacial faults. Quaternary Science Reviews 19: 1447-1460

Dehls JF, Olesen O, Bungum H, Hicks EC, Lindholm CD, Riis F (2000b) Neotectonic map: Norway and adjacent areas. Scale 1:3 million. Geological Survey of Norway, Trondheim

Devoli G, Eikenæs O, Taurisano A, Hermanns RL, Fischer L, Oppikofer T, Bunkholt H (2011) Plan for skredfarekartlegging - Delrapport steinsprang steinskred og fjellskred. NVE rapport 15/2011. Norges Vassdrags-og Energidirektorat, Oslo, Norway (in Norwegian 120 pp.)

Dowdeswell JA, Ottesen D, Rise L (2010) Rates of sediment delivery from the Fennoscandian Ice Sheet through an ice age. Geology 38: 3–6

Eisbacher GH, Clague JJ (1984) Destructive mass movements in high mountains: Hazard and management. Geological Survey of Canada Paper 84–16

Etzelmüller B, Romstad B, Fjellanger J (2007) Automatic regional classification of topography in Norway. Norwegian Journal of Geology 87: 167–180

Evans SG, Clague JJ (1994) Recent climatic change and catastrophic geomorphic processes in mountain environments. Geomorphology 10: 107–128

Evans SG, Clague JJ, Woodsworth GJ, Hungr O (1989) The Pandemonium Creek rock avalanche, British Columbia. Canadian Geotechnical Journal 26: 427–446

Fenton CR, Hermanns RL, Blikra LH, Kubik PW, Bryant C, Niedermann S, Meixner A, Goethals MM (2011) Regional ^{10}Be production rate calibration for the past 12 ka deduced from the radiocarbon-dated Grøtlandsura and Russenes rock avalanches at 69° N, Norway. Quaternary Geochronology 6: 437-452

Fischer L, Kääb A, Huggel C, Noetzli J (2006) Geology, glacier retreat and permafrost degradation as controlling factors of slope instabilities in a high-mountain rock wall: the Monte Rosa east face. Natural Hazards and Earth System Science 6: 761-772

Fjeldskaar W (1997) Flexural rigidity of Fennoscandia inferred from the postglacial uplift. Tectonics 16: 596-608

Fjeldskaar W, Lindholm C, Dehls JF, Fjeldskaar I (2000) Post-glacial uplift, neotectonics and seismicity in Fennoscandia. Quaternary Science Reviews 19: 1413–1422

Furseth A (2006) Skredulykker i Norge. Tun Forlag, Oslo, Norway (in Norwegian 207 pp.)

Gardner JS (1980) Frequency magnitude and spatial distribution of mountain rockfalls and rockslides in the Highwood Pass area, Alberta, Canada. In: Coates DR, Vitek JD (eds) Thresholds in Geomorphology. Allen and Unwin, London, pp. 267–295

Gariano SL, Guzzetti F (2016) Landslides in a changing climate. Earth-Science Reviews 162: 227–252

Gee DG, Sturt BA (eds) (1985) The Caledonide orogen–Scandinavia and related areas. Volume 1. Wiley, Chichester

Gisnås K, Etzelmüller B, Farbrot H, Schuler TV, Westermann S (2013) Cryo-GRID 1.0: Permafrost Distribution in Norway estimated by a Spatial Numerical Model. Permafrost and Periglacial Processes 24: 2–19

Gisnås K, Westermann S, Schuler TV, Melvold K, Etzelmüller B (2016) Small-scale variation of snow in a regional permafrost model. The Cryosphere 10: 1201-1215

Goering BM, Lohne ØL, Mangerud J, Svendsen JI, Gyllencreutz R, Schaefer J, Finkel R (2012) Late Glacial and Holocene ^{10}Be production rates for western Norway. Journal of Quaternary Science 27: 89-96

Gjessing J (1967) Norway's paleic surface. Norsk Geografisk Tidsskrift 21: 69–132

Grämiger LM, Moore JR, Gischig VS, Ivy-Ochs S, Loew S (2017) Beyond debuttressing: Mechanics of paraglacial rock slope damage during repeat glacial cycles. Journal of Geophysical Research: Earth Surface 122: 1004–1036

Grämiger LM, Moore JR, Gischig VS, Loew S (2018) Thermomechanical Stresses Drive Damage of Alpine Valley Rock Walls During Repeat Glacial Cycles. Journal of Geophysical Research: Earth Surface 123: 2620–2646

Grimstad E, Nesdal S (1990) The Loen rockslides - a historical review. In: Barton M, Stephansson W (eds) Rock Joints: Proceedings of the International Symposium on rock joints, Loen, Norway, 4-6 June 1990. Balkema, Rotterdam, pp. 3-8

Grove JM (1972) The incidence of landslides, avalanches, and floods in western Norway during the Little Ice Age. Arctic and Alpine Research 4: 131–138

Hammer KM, Smith ND (1983) Sediment production and transport in a proglacial stream: Hilda Glacier, Alberta, Canada. Boreas 12: 91–106

Hansen L, Beylich A, Burki V, Eilertsen RS, Fredin O, Larsen E, Lysså E, Nesje A, Stalsberg K, Tønnesen JF (2009) Stratigraphic architecture and infill history of a deglaciated bedrock valley based on georadar, seismic profiling and drilling. Sedimentology 56: 1751–1773

Hanssen-Bauer I, Førland EJ, Haddeland I, Hisdal H, Lawrence D, Mayer S, Nesje A, Nilsen JEØ, Sandven S, Sandø AB, Sorteberg A, Ådlandsvik B (2017) Climate in Norway 2100 - a knowledge base for climate adaptation. Rapport No. 1/2017. The Norwegian Centre for Climate Services, Oslo

Harbitz CB, Glimsdal S, Løvholt F, Kveldsvik V, Pedersen GK, Jensen A (2014) Rockslide tsunamis in complex fjords: from an unstable rock slope at Åkerneset to tsunami risk in western Norway. Coastal Engineering 88: 101–122

Henderson IHC, Saintot A (2011) Regional spatial variations in rockslide distribution from structural geology ranking: an example from Storfjorden, western Norway. In: Jaboyedoff M (ed) Slope Tectonics. Geological Society, London, Special Publications 351, pp. 79–95

Hermanns RL, Longva O (2012) Rapid rock slope failures. In: Clague JJ, Stead D (eds) Landslides: Types, Mechanisms, and Modelling. Cambridge University Press, Cambridge, pp. 59–70

Hermanns RL, Blikra LH, Naumann M, Nilsen B, Panthi KK, Stromeyer D, Longva O (2006a) Examples of multiple rock-slope collapses from Köfels (Ötz valley, Austria) and western Norway. Engineering Geology 83: 94–108

Hermanns RL, Niedermann S, Garcia AV, Schellenberger A (2006b) Rock avalanching in the NW Argentine Andes as a result of complex interactions of lithologic, structural and topographic boundary conditions, climate change and active tectonics. In: Evans SG, Scarawcia Mugnozza G, Strom AL, Hermanns RL (eds) Landslides from Massive Rock Slope Failure: Proceedings of the NATO Advanced Research Workshop on Massive Rock Slope Failure: New Models for Hazard Assessment, Celano, Italy, 16-21 June 2002, (NATO Science Series: IV, Earth and Environmental Sciences; 49). Springer, Dordrecht, pp. 497–520

Hermanns RL, Blikra LH, Ivy-Ochs S, Kubik P, Naumann R (2009) Geomorphic control on the size of outburst floods: Examples from Tafjord, Norway and Patagonia. In: Nakrem HA (ed) Proceedings of Vinterkonferansen, Norsk Geologisk Forening, Bergen, pp. 50-51

Hermanns RL, Fischer L, Oppikofer T, Bøhme M, Dehls JF, Henriksen H, Booth A, Eilertsen R, Longva O, Eiken T (2011) Mapping of unstable and potentially unstable rock slopes in Sogn og Fjordane (work report 2008-2010). NGU Rapport 2011.055. Geological Survey of Norway, Trondheim, Norway

Hermanns RL, Redfield T, Bunkholt H, Fischer L, Oppikofer T, Gosse J, Eiken T (2012) Cosmogenic nuclide dating of slow moving rockslides in Norway in order to assess long-term slide velocities. In: Eberhardt E, Froese C, Turner K, Leroueil S (eds) Landslides and Engineered Slopes. Protecting Society through Improved Understanding: Proceedings of the 11th International and 2nd North American Symposium on Landslides, Banff, Canada, 3-8 June 2012. Balkema, Rotterdam, pp. 3-8

Hermanns RL, Oppikofer T, Anda E, Blikra LH, Böhme M, Bunkholt H, Crosta GB, Dahle H, Devoli G, Fischer L, Jaboyedoff M, Loew S, Sætre S, Yugsi Molina FX (2013a) Hazard and risk classification for large unstable rock slopes in Norway. Proceedings of the International Conference on Vaiont 1963–2013 - Thoughts and Analyses after 50 Years

since the Catastrophic Landslide. Italian Journal of Engineering Geology and Environment - Book Series 6. Sapienza University, Rome, pp. 245–254

Hermanns RL, Oppikofer T, Dahle H, Eiken T, Ivy-Ochs S, Blikra LH (2013b) Understanding long-term slope deformation for stability assessment of rock slopes: the case of the Oppstadhornet rockslide, Norway. Proceedings of the International Conference on Vaiont, 1963–2013 - Thoughts and Analyses after 50 Years since the Catastrophic Landslide. Italian Journal of Engineering Geology and Environment - Book Series 6. Sapienza University, Rome, pp. 255–264

Hermanns R, Blikra L, Anda E, Saintot A, Dahle H, Oppikofer T, Fischer L, Bunkholt H, Böhme M, Dehls J, Lauknes T, Redfield T, Osmundsen P, Eiken T (2013c) Systematic mapping of large unstable rock slopes in Norway. In: Margottini C, Canuti P, Sassa K (eds) Landslide Science and Practice, Volume 1: Landslide Inventory and Susceptibility and Hazard Zoning. Springer-Verlag, Heidelberg, pp. 29–34

Hermanns RL, Schleier M, Böhme M, Blikra LH, Gosse K, Ivy-Ochs S, Hilger P (2017a) Rock-Avalanche Activity in W and S Norway Peaks After the Retreat of the Scandinavian Ice Sheet. In: Mikoš M, Vilímek V, Yin Y, Sassa K (eds) Advancing Culture of Living with Landslides, Volume 5: Landslides in Different Environments. Springer-Verlag, Heidelberg, pp. 331-338

Hermanns RL, Böhme M, Oppikofer T, Gosse J, Penna IM (2017b) When does progressive rock-slope failure start and how does it develop in time? An analysis from Norway: a landscape dominated by steep alpine relief excavated by multiple glacial cycles. In: Leith K, Ziegler M, Perras M, Loew S (eds) Progressive Rock Failure Conference, Monte Verità, 5–9 June 2017, Extended Abstracts. ETH Zurich, Zurich, pp. 40-43

Hewitt K (2002) Introduction: Landform Assemblages and Transitions in Cold Regions. In: Hewitt K, Byrne M-L, English M, Young G (eds) Landscapes of Transition: Landform Assemblages and Transformations in Cold Regions. Springer, Dordrecht, pp. 1-8

Hewitt K (2006) Disturbance regime landscapes: mountain drainage systems interrupted by large rockslides. Progress in Physical Geography 30: 365-393

Hilger P, Hermanns RL, Gosse JC, Jacobs B, Etzelmüller B, Krautblatter M (2018) Multiple rock-slope failures from Mannen in Romsdal Valley, western Norway, revealed from Quaternary geological mapping and ^{10}Be exposure dating. The Holocene 28: 1841-1854

Hinchliffe S, Ballantyne CK (1999) Talus accumulation and rockwall retreat, Trotternish, Isle of Skye Scotland. Scottish Geographical Journal 115: 53-70

Hipp T, Etzelmüller B, Westermann S (2014) Permafrost in Alpine Rock Faces from Jotunheimen and Hurrungane, Southern Norway. Permafrost and Periglacial Processes 25: 1–13

Holm K, Bovis M, Jakob M (2004) The landslide response of alpine basins to post-Little Ice Age glacial thinning and retreat in southwestern British Columbia. Geomorphology 57: 201–216

Hughes ALC, Gyllencreutz R, Lohne ØS, Mangerud J, Svendsen JI (2016) The last Eurasian ice sheets – a chronological database and time-slice reconstruction, DATED-1. Boreas 45: 1–45

Hungr O, Leroueil S, Picarelli L (2014) The Varnes classification of landslide types, an update. Landslides 11: 167–194

Jaboyedoff M, Derron M, Jakubowski J, Oppikofer T, Pedrazzini A (2012) The 2006 Eiger rockslide, European Alps. In: Clague JJ, Stead D (eds) Landslides: Types, Mechanisms and Modeling. Cambridge University Press, Cambridge, pp. 282-296

Jarman D (2006) Large rock slope failures in the Highlands of Scotland: characterisation, causes and spatial distribution. Engineering Geology 83: 161–182

Jarman D (2009) Paraglacial rock slope failure as an agent of glacial trough widening. In: Knight J, Harrison S (eds) Periglacial and Paraglacial Processes and Environments. Geological Society, London, Special Publications 320, pp. 102-131

Jarman D, Ballantyne CK (2002) Beinn Fhada, Kintail: a classic example of paraglacial rock-slope deformation. Scottish Geographical Journal 118: 59–68

Jarman D, Harrison S (2019) Rock slope failure in the British mountains. Geomorphology 340: 202-233

Jibson RW (1996) Using Landslides for Paleoseismic Analysis. In: McCalpin JP (ed) Paleoseismology. Academic Press, San Diego, International Geophysics Series 62, pp. 397-438

Johnson PG (1984) Paraglacial conditions of instability and mass movement: a discussion. Zeitschrift für Geomorphologie 28: 235–250

Karlen W, Matthews JA (1992) Reconstructing Holocene glacier variations from glacial lake sediments: studies from Nordvestlandet and Jostedalsbreen-Jotunheimen, southern Norway. Geografiska Annaler 74A: 327-348

Keefer DK (1984) Landslides caused by earthquakes. Geological Society of America, Bulletin 95: 406–421

Kirkbride MP, Deline P (2018) Spatial heterogeneity in the paraglacial response to post-Little Ice Age deglaciation of four headwater cirques in the Western Alps. Land Degradation & Development 29: 3127–3140

Knapp S, Gilli A, Anselmetti FS, Krautblatter M, Hajdas I (2018) Multistage rock-slope failures revealed in lake sediments in a seismically active Alpine region (Lake Oeschinen, Switzerland). Journal of Geophysical Research: Earth Surface 123: 658–677

Knight J, Harrison S (2014) Mountain glacial and paraglacial environments under global climate change: lessons from the past, future directions and policy implications. Geografiska Annaler 96A: 245-264

Knight J, Harrison S (2018) Transience in cascading paraglacial systems. Land Degradation and Development 29: 1991-2001

Kos A, Amann F, Strozzi T, Delaloye R, von Ruette J, Springman S (2016) Contemporary glacier retreat triggers a rapid landslide response, Great Aletsch Glacier, Switzerland. Geophysical Research Letters 43(24): 12466-12474

Krautblatter M, Huggel C, Deline P, Hasler A (2012) Research perspectives on unstable high-alpine bedrock permafrost: measurement, modelling and process understanding. Permafrost and Periglacial Processes 23: 80–88

Krautblatter M, Funk D, Günzel FK (2013) Why permafrost rocks become unstable: A rock-ice-mechanical model in time and space. Earth Surface Processes and Landforms 38: 876–887

Lal D (1991) Cosmic ray labeling of erosion surfaces: in situ nuclide production rates and erosion models. Earth and Planetary Science Letters 104: 424–439

Laute K, Beylich AA (2013) Holocene hillslope development in glacially formed valley systems in Nordfjord, western Norway. Geomorphology 188: 12–30

Leith K, Amann F, Moore JR, Kos A, Loew S (2010a) Conceptual modelling of near-surface extensional fracture in the Matter and Saas Valleys, Switzerland. In: Williams AL, Pinches GM, Chin CY, McMorran TJ, Massey CI (eds) Geologically Active: Proceedings of the 11th IAEG Congress, Auckland, New Zealand. CRC Press, Boca Raton, pp. 363e371

Leith K, Moore J, Amann F, Loew S (2010b) Slope failure induced by post-glacial extensional fracturing in the Matter and Saas Valleys, Switzerland. Geophysical Research Abstracts 12 (EGU2010-4599)

Lepland A, Bøe R, Sønstegaard E, Haflidason H, Hovland C, Olsen H, Sandnes R (2002) Sedimentological descriptions and results of analytical tests of sediment cores from fjords

and lakes in northwest Western Norway. NGU Rapport 2002.014. Geological Survey of Norway, Trondheim, Norway

Lifton N, Sato T, Dunai TJ (2014) Scaling in situ cosmogenic nuclide production rates using analytical approximations to atmospheric cosmic-ray fluxes. Earth and Planetary Science Letters 386: 149–160

Lilleøren K, Etzelmüller B (2011) A regional inventory of rock glaciers and ice-cored moraines in Norway. Geografiska Annaler 93A: 175–191

Lilleøren KS, Etzelmüller B, Schuler TV, Ginås K, Humlum O (2012) The relative age of permafrost – estimation of Holocene permafrost limits in Norway. Global and Planetary Change 92–93: 209–223

Lohne ØS, Mangerund J, Birks HH (2013) Precise ^{14}C ages of the Vedde and Saksunarvatn ashes and the Younger Dryas boundaries from western Norway and their comparison with the Greenland Ice Core (GICC05) chronology. Journal of Quaternary Science 28: 490–500

Longva O, Blikra LH, Dehls JF (2009) Rock avalanches - distribution and frequencies in the inner part of Storfjorden, Møre og Romsdal County, Norway. NGU Rapport 2009.002. Geological Survey of Norway, Trondheim, Norway

Mangerud J (2004) Ice sheet limits on Norway and the Norwegian continental shelf. In: Ehlers J, Gibbard PL (eds) Quaternary Glaciations – Extent and Chronology. Volume 1: Europe. Elsevier, Amsterdam, pp. 271–294

Mangerud J, Gyllencreutz R, Lohne Ø, Svendsen JI (2011) Glacial History of Norway. In: Ehlers J, Gibbard PL, Hughes PD (eds) Developments in Quaternary Science Volume 15. Elsevier Amsterdam, pp. 279-298

Marion J, Filion L, Hétu B (1995) The Holocene development of a debris slope in subarctic Québec, Canada. The Holocene 5: 409–419

Marr P, Winkler S, Löffler J (2019) Schmidt-hammer exposure-age dating (SHD) performed on periglacial and related landforms in Opplendskedalen, Geirangerfjellet, Norway: Implications for mid- and late-Holocene climate variability. The Holocene 29: 97-109

Matthews JA, Wilson P (2015) Improved Schmidt-hammer exposure ages for active and relict pronival ramparts in southern Norway, and their palaeoenvironmental implications. Geomorphology 246: 7–21

Matthews JA, Nesje A, Linge H (2013) Relict Talus-Foot Rock Glaciers at Øyberget, Upper Ottadalen, Southern Norway: Schmidt Hammer Exposure Ages and Palaeoenvironmental Implications. Permafrost and Periglacial Processes 24: 336-346

Matthews JA, Wilson P, Mourne RW (2017) Landform transitions from pronival ramparts to moraines and rock glaciers: a case study from the Smørbotn cirque, Romsdalsalpane, southern Norway. Geografiska Annaler 99A: 15-37

Matthews JA, Winkler S, Wilson P, Tomkins MD, Dortch JM, Mourne RW, Hill JL, Owen G, Vater AE (2018) Small rock-slope failures conditioned by Holocene permafrost degradation: a new approach and conceptual model based on Schmidt-hammer exposure-age dating, Jotunheimen, southern Norway. Boreas 47: 1144–1169

McColl ST (2012) Paraglacial rock-slope stability. Geomorphology 153–154: 1–16

McColl ST, Davies TRH (2013) Large ice-contact slope movements: glacial buttressing, deformation and erosion. Earth Surface Processes and Landforms 38: 1102–1115

McColl ST, Draebing D (2019) Rock Slope Instability in the Proglacial Zone: State of the Art. In: Heckman T, Morche D (eds) Geomorphology of Proglacial Systems: Landform and Sediment. Springer, Cham, pp. 119-141

McSaveney MJ (1993) Rock avalanches of 2 May and 6 September 1992, Mount Fletcher, New Zealand. Landslide News 7: 2–4

Mercier D, Cossart E, Decaulne A, Feuillet T, Jónsson HP, Sæmundsson Þ (2013) The Höfðahólar rock avalanche (sturzström): Chronological constraint of paraglacial landsliding on an Icelandic hillslope. The Holocene 23: 432–446

Messenzehl K, Meyer H, Otto J-C, Hoffmann T, Dikau R (2017) Regional-scale controls on the spatial activity of rockfalls (Turtmann Valley, Swiss Alps) - A multivariate modeling approach. Geomorphology 287: 29-45

Mörner N-A (2005) An interpretation and catalogue of palaeoseismicity in Sweden. Tectonophysics 408: 265-307

Mörner N-A (2013) Patterns in seismology and palaeoseismology and their application in long-term hazard assessments – the Swedish case in view of nuclear waste management. Pattern Recognition in Physics 1: 75–89

Murton JB, Peterson R, Ozouf J-C (2006) Bedrock fracture by ice segregation in cold regions. Science 314: 1127–1129

Nesje A (2002) A large rockfall avalanche in Oldedalen, inner Nordfjord, western Norway, dated by means of a sub-avalanche Salix sp. tree trunk. Norwegian Journal of Geology 82: 59-62

Nesje A (2009) Latest Pleistocene and Holocene alpine glacier fluctuations in Scandinavia. Quaternary Science Reviews 28: 2119–2136

Nesje A, Kvamme M, Rye N, Løvlie R (1991) Holocene glacial and climate history of the Jostedalsbreen region, western Norway: evidence from lake sediments and terrestrial deposits. Quaternary Science Reviews 10: 87–114

Nesje A, Blikra LH, Anda E (1994) Dating rockfall-avalanche deposits from degree of rock-surface weathering by Schmidt-hammer tests: a study from Norangsdalen, Sunnmøre, Norway. Norwegian Journal of Geology 74: 108-113

Nesje A, Matthews JA, Dahl SO, Berrisford M, Andersson C (2001) Holocene glacier fluctuations of Flatebreen and winter-precipitation changes in the Jostedalsbreen region, western Norway, based on glaciolacustrine sediment records. The Holocene 11: 267-280

Nesje A, Bakke J, Dahl SO, Lie Ø, Matthews JA (2008) Norwegian mountain glaciers in the past, present and future. Global and Planetary Change 60: 10-27

NGU (2015) Bedrock – national bedrock database. Geological Survey of Norway. Available at: http://geo.ngu.no/kart/berggrunn_mobil/ (accessed 17 June 2019) [in Norwegian]

NVE (2018) NVE Atlas. Available at: https://atlas.nve.no/ (accessed 17 June 2019) [in Norwegian]

Olesen O, Blikra LH, Braathen A, Dehls JF, Olsen L, Rise L, Roberts D, Riis F, Faleide JI, Anda E (2004) Neotectonic deformation in Norway and its implications: a review. Norwegian Journal of Geology 84: 3-34

Olesen O, Bungum H, Dehls J, Lindholm C, Pascal C, Roberts D (2013) Neotectonics seismicity and contemporary stress field in Norway – mechanisms and implications. In: Olsen L, Fredin O, Olesen O (eds) Quaternary Geology of Norway. Geological Survey of Norway Special Publication 13, Trondheim, pp. 145–174

Oliva M, Mercier D, Ruiz-Fernández J, McColl S (2019) Paraglacial processes in recently deglaciated environments. Land Degradation and Development, in press

Olsen L, Sveian H, Bergstrøm B, Ottesen D, Rise L (2013) Quaternary glaciations and their variations in Norway and on the Norwegian continental shelf. In: Olsen L, Fredin O, Olesen O (eds) Quaternary Geology of Norway. Geological Survey of Norway Special Publication 13, Trondheim, pp. 27–78

Oppikofer T, Saintot A, Otterå S, Hermanns RL, Anda E, Dahle H, Eiken T (2013) Investigations on unstable rock slopes in Møre og Romsdal – status and plans after field surveys in 2012. NGU Rapport 2013.014. Geological Survey of Norway, Trondheim, Norway

Oppikofer T, Nordahl B, Bunkholt H, Nicolaisen M, Jarna A, Iversen S, Hermanns RL, Böhme M, Yugsi Molina FX (2015) Database and online map service on unstable rock

slopes in Norway - from data perpetuation to public information. Geomorphology 249: 69–81

Oppikofer T, Hermanns RL, Sandøy G, Böhme M, Jaboyedoff M, Horton P, Roberts NJ, Fuchs H (2016) Quantification of casualties from potential rock-slope failures in Norway. In: Aversa S, Cascini L, Picarelli L, Scavia C (eds) Landslides and Engineered Slopes. Experience, Theory and Practice: Proceedings of the 12th International Symposium on Landslides (Napoli, Italy, 12-19 June 2016). CRC Press/Balkema, Leiden, pp. 1537-1544

Oppikofer T, Saintot A, Hermanns RL, Böhme M, Scheiber T, Gosse J, Dreiås GM (2017) From incipient slope instability through slope deformation to catastrophic failure — Different stages of failure development on the Ivasnasen and Vollan rock slopes (western Norway). Geomorphology 289: 96-116

Ostermann M, Sanders D (2017) The Benner pass rock avalanche cluster suggests a close relation between long-term slope deformation (DSGSDs and translational rock slides) and catastrophic failure. Geomorphology 289: 44–59

Pánek T, Klimeš J (2016) Temporal behavior of deep-seated gravitational slope deformations: a review. Earth Science Reviews 156: 14–38

Peulvast J-P (1985) Relief, érosion différentielle et morphogenèse dans un bourrelet montagneux de haute latitude: Lofoten-vesteralen et Sogn-Jotun (Norvège). Unpublished Ph.D. thesis, University of Paris 1 Panthéon-Sorbonne, Paris, 1642 pp

Phillips JD (2003) Sources of nonlinearity and complexity in geomorphic systems. Progress in Physical Geography 27: 1–23

Prager C, Zangerl C, Patzelt G, Brandner R (2008) Age distribution of fossil landslides in the Tyrol (Austria) and its surrounding areas. Natural Hazards and Earth Systems Science 8: 377-407

Radbruch-Hall DH (1978) Gravitational creep of rock masses on slopes. In: Voight B. (ed) Rockslides and Avalanches, Volume 1: Natural Phenomena. Elsevier, Amsterdam, pp. 607–657

Redfield TF, Hermanns RL (2016) Gravitational slope deformation, not neotectonics: Revisiting the Nordmannvikdalen feature of northern Norway. Norwegian Journal of Geology 96: 245-273

Reimer PJ, Bard E, Bayliss A, et al (2013) IntCal13 and Marine13 Radiocarbon Age Calibration Curves 0–50,000 Years cal BP. Radiocarbon 55: 1869–1887

Riva F, Agliardi F, Amitrano D, Crosta GB (2018) Damage-based time-dependent modeling of paraglacial to postglacial progressive failure of large rock slopes. Journal of Geophysical Research: Earth Surface 123: 124-141

Rodríguez-Rodríguez L, González-Lemos S, Ballesteros D, Valenzuela P, Domínguez-Cuesta MJ, Llana-Fúnez S, Jiménez-Sánchez M (2018) Timing of paraglacial rock-slope failures and denudation signatures in the Cantabrian Mountains (North Iberian Peninsula). Land Degradation and Development 29: 3159–3173

Ryder JM (1971) The stratigraphy and morphology of paraglacial alluvial fans in south-central British Columbia. Canadian Journal of Earth Science 8: 279–298

Rye N, Nesje A, Lien R, Anda E (1987) The late Weichselian ice sheet in the Nordfjord-Sunnmøre area and deglaciation chronology for Nordfjord, western Norway. Norsk Geografisk Tidsskrift 41: 23-43

Saintot A, Henderson IHC, Derron M-H (2011) Inheritance of ductile and brittle structures in the development of large rock slope instabilities: examples from western Norway. In: Jaboyedoff M (ed) Slope Tectonics. Geological Society, London, Special Publications 351, pp. 27-78

Sandøy G, Oppikofer T, Nilsen B (2017) Why did the 1756 Tjellefonna rockslide occur? A back-analysis of the largest historic rockslide in Norway. Geomorphology 289: 78–95

Schleier M, Hermanns RL, Rohn J, Gosse J (2015) Diagnostic characteristics and paleodynamics of supraglacial rock avalanches, Innerdalen, Western Norway. Geomorphology 245: 23–39

Schleier M, Hermanns RL, Krieger I, Oppikofer T, Eiken T, Rønning JS, Rohn J (2016) Gravitational reactivation of a pre-existing post-Caledonian fault system: the deep-seated gravitational slope deformation at Middagstinden, western Norway. Norwegian Journal of Geology 96: 201–222

Schleier M, Hermanns RL, Gosse JC, Oppikofer T, Rohn J, Tønnesen AF (2017) Subaqueous rock-avalanche deposits exposed by post-glacial isostatic rebound, Innfjorddalen, Western Norway. Geomorphology 289: 117–133

Sigurdsson O, Williams RS (1991) Rockslides on the terminus of 'Jökulsárgilsjökull', southern Iceland. Geografiska Annaler 73A: 129–140

Slaymaker O (2009) Proglacial, periglacial or paraglacial? In: Knight J, Harrison S (eds) Periglacial and Paraglacial Processes and Environments. Geological Society, London, Special Publications 320, pp. 71–84

Slaymaker O (2011) Criteria to distinguish between periglacial, proglacial and paraglacial environments. Quaestiones Geographicae 30: 85–94

Sollid JL, Sørbel L (1979) Deglaciation of western Central Norway. Boreas 8: 233–239

Steiger C, Etzelmüller B, Westermann S, Myhra KS (2016) Modelling the permafrost distribution in steep rock walls in Norway. Norwegian Journal of Geology 96: 329–341

Stewart IS, Sauber J, Rose J (2000) Glacio-seismotectonics: ice sheets, crustal deformation and seismicity. Quaternary Science Reviews 19: 1367–1389

Stone J (2000) Air pressure and cosmogenic isotope production. Journal of Geophysical Research 105: 23753–23760

Svendsen JI, Mangerud J (1987) Late Weichselian and Holocene sea-level history for a cross-section of western Norway. Journal of Quaternary Science 2: 113–132

Tibaldi A, Rovida A, Corazzato C (2004) A giant deep-seated slope deformation in the Italian Alps studied by paleoseismological and morphometric techniques. Geomorphology 58: 27–47

Tveten E, Lutro O, Thorsnes T (1998) Geologisk kart over Norge, 1:250,000. Geological Survey of Norway, Trondheim, Norway

Vestøl O (2006) Determination of postglacial land uplift in Fennoscandia from levelling, tide-gauges and continuous GPS stations using least squares collocation. Journal of Geodesy 80: 248–258

Wilson P (2009) Rockfall talus slopes and associated talus-foot features in the glaciated uplands of Great Britain and Ireland: periglacial, paraglacial or composite landforms? In: Knight J, Harrison S (eds) Periglacial and Paraglacial Processes and Environments. Geological Society, London, Special Publications 320, pp. 133-144

Wilson P (2017) Periglacial and paraglacial processes, landforms and sediments. In: Coxon P, McCarrron S, Mitchell F (eds) Advances in Irish Quaternary Studies, Volume 1. Atlantis Press, Paris, pp. 217-254

Winkler S (20XX) Terminal moraine formation processes and geomorphology of glacier forelands at selected outlet glaciers of Jostedalsbreen, South Norway. In: Beylich AA (ed) Landscapes and Landforms of Norway. Springer, Dordrecht, pp. XXX-XXX

Winsvold SH, Andreassen LM, Kienholz C (2014) Glacier area and length changes in Norway from repeat inventories. The Cryosphere 8: 1885–1903

Wyrwoll K-H (1977) Causes of rock-slope failure in a cold area: Labrador-Ungava. Geological Society of America Reviews in Engineering Geology 3: 59–67

Index